

Activity of liposomal taxol against breast cancer cells

by

Melanie Heney

Department of Biology

Submitted in partial fulfillment of the requirements
for the Master's degree

Faculty of Graduate Studies
Lakehead University
Thunder Bay, Ontario

July 13, 2007

© Melanie Heney



Library and
Archives Canada

Bibliothèque et
Archives Canada

Published Heritage
Branch

Direction du
Patrimoine de l'édition

395 Wellington Street
Ottawa ON K1A 0N4
Canada

395, rue Wellington
Ottawa ON K1A 0N4
Canada

Your file *Votre référence*
ISBN: 978-0-494-33578-9
Our file *Notre référence*
ISBN: 978-0-494-33578-9

NOTICE:

The author has granted a non-exclusive license allowing Library and Archives Canada to reproduce, publish, archive, preserve, conserve, communicate to the public by telecommunication or on the Internet, loan, distribute and sell theses worldwide, for commercial or non-commercial purposes, in microform, paper, electronic and/or any other formats.

The author retains copyright ownership and moral rights in this thesis. Neither the thesis nor substantial extracts from it may be printed or otherwise reproduced without the author's permission.

AVIS:

L'auteur a accordé une licence non exclusive permettant à la Bibliothèque et Archives Canada de reproduire, publier, archiver, sauvegarder, conserver, transmettre au public par télécommunication ou par l'Internet, prêter, distribuer et vendre des thèses partout dans le monde, à des fins commerciales ou autres, sur support microforme, papier, électronique et/ou autres formats.

L'auteur conserve la propriété du droit d'auteur et des droits moraux qui protègent cette thèse. Ni la thèse ni des extraits substantiels de celle-ci ne doivent être imprimés ou autrement reproduits sans son autorisation.

In compliance with the Canadian Privacy Act some supporting forms may have been removed from this thesis.

Conformément à la loi canadienne sur la protection de la vie privée, quelques formulaires secondaires ont été enlevés de cette thèse.

While these forms may be included in the document page count, their removal does not represent any loss of content from the thesis.

Bien que ces formulaires aient inclus dans la pagination, il n'y aura aucun contenu manquant.


Canada

Table of Contents

Acknowledgments	5
Abstract	6
I. Introduction	8
Chapter 1: Chemotherapy and Paclitaxel.....	8
1.1 History of Paclitaxel	8
1.2 Chemical Nature of Taxol	9
Figure 1: Chemical structure of taxol	9
1.3 Mechanism of Action.....	9
Figure 2: The binding of taxol to microtubules	10
Figure 3: Brightfield microscopy demonstrating the effects of taxol.....	11
1.4 Pre-clinical Trials.....	11
1.5 Clinical Trials	12
Figure 4: Flow chart depicting the steps of drug development	14
1.6 Chemotherapeutic use in Clinic.....	14
1.7 Current Formulation of Taxol	15
1.8 Recent Developments	16
Chapter 2: Drug Resistance	17
2.1 Models of Drug Resistance	17
Figure 5: Cellular factors that cause drug resistance	18
2.2 Mechanisms of Taxol Resistance.....	19
Figure 6: P-glycoprotein efflux pump	20
2.3 Measuring Drug Resistance and Apoptosis	22
2.4 Strategies to Overcome Resistance	25
Chapter 3: Liposomes	26
3.1 Liposomes	26
Figure 7: Internalization of fluorescently-tagged liposomes.....	27
3.2 Structure and Composition of Liposomes	27
Figure 8: The chemical structure of lipids used in this study	28
3.3 Targeting Liposomes.....	29

3.4 The EPR effect.....	29
3.5 Liposomal Encapsulation of Anticancer Agents	30
3.6 Other Liposomal Treatments.....	31
3.7 Liposomal Taxol	33
II. Summary	34
III. Objectives of the Project	35
IV. Materials and Methods	37
Part 1: Establishment of a taxol-resistant MCF-7 clone	37
4.1 Propagation of Cultured Cell Lines	37
Table 1. A summary of cell lines used in the study.....	38
4.2 Treatment of Cells	38
4.3 Doubling Time Analysis.....	38
4.4 Establishing an MCF-7 Taxol-resistant Cell Line (clone)	39
Figure 9: Flow chart of method for establishing clone	40
4.5 Colony Formation Assay	40
Figure 10: Flow chart of colony formation assay methodology.....	42
4.6 Standardization of the MTT Cytotoxicity Assay.....	42
4.7 MTT <i>in vitro</i> Cytotoxicity Assay	43
Part 2: Characterization of Liposomes	43
4.8 Preparation of Liposomal Paclitaxel	43
4.9 Quantification of Taxol	44
4.10 Drug Release Study.....	45
4.11 Rehydration of Liposomal Taxol	45
4.12 Toxicity of Liposomes	46
Part 3: Evaluation of the effects of CrEL vs. liposomal taxol.....	46
4.13 DNA Isolation.....	46
4.14 DNA Fragmentation Assay	47
4.15 Flow Cytometric Cell Cycle Analysis of Taxol-treated Cells	47
4.16 Determination of Mitotic Index.....	48
4.17 UPLC Analysis of Relative Taxol Uptake	49
4.18 MTT Analysis of the Role of Caspases in Taxol-induced Apoptosis.....	50
4.19 Western Blot Analysis of P-gp in MCF-7 Cells.....	51

4.20 Statistical Analysis	51
V. Results.....	52
Part 1: Establishing a taxol-resistant MCF-7 clone.....	52
Figure 11: Cell growth rates of MCF-7 cells.....	54
Table 2: Doubling time comparison	54
Figure 12: Colonization assay	55
Figure 13: Standard curves to optimize MTT assay.....	57
Table 3: Optimal plating densities for MTT assay	57
Figure 14: MTT analysis of MCF-7 cells	58
Table 4: IC ₅₀ values for 4-day taxol treatment	58
Part 2. Characterization of Liposomes.....	59
Table 5: Liposomal formulations used in this study	60
Figure 15: Cumulative release of taxol from liposomes	60
Figure 16: Stability of liposomal taxol.....	61
Figure 17: Size distribution of DPPC:DMPG liposomes.....	62
Table 5: Size distribution and encapsulation efficiency of liposomal taxol.....	62
Figure 18: MTT analysis of cytotoxicity of empty DPPC: DMPG liposomes.....	63
Part 3: Evaluation of the effects of CrEL vs. liposomal taxol	64
Table 6a: Flow cytometric analysis of the cell cycle of wild-type A MCF-7 cells	65
Table 6b: Flow cytometric analysis of the cell cycle of clone MCF-7 cells	65
Table 6c: Flow cytometric analysis of the cell cycle of tax-resistant MCF-7 cells	66
Figure 19a: Histograms of flow cytometry data for wild-type A MCF-7 cells.	67
Figure 19b: Histograms of flow cytometry data for clone MCF-7 cells.....	68
Figure 19c: Histograms of flow cytometry data for tax-resistant MCF-7 cells.....	69
Table 7: Mitotic indexes of control and taxol-treated MCF-7 cells	71
Figure 20: Fluorescent microscopy demonstrating mitotic arrest.....	71
Figure 21a: DNA laddering gel demonstrating DNA fragmentation	73
Figure 21b: Mean CNT density values for DNA laddering samples	74
Figure 22: UPLC chromatogram showing taxol uptake	76
Table 8: Values for taxol uptake determined by UPLC analysis.....	77
Figure 23: Western blot analysis of P-glycoprotein expression in MCF-7 cells	79

Figure 24: MTT analysis of the effect of caspase inhibitors and taxol treatment on MCF-7 cells	80
Figure 25: Standard curves to optimize MTT cytotoxicity assay for A549 cells.....	82
Table 9: Optimal plating densities for MTT analysis of A549 lung cancer cells.....	82
Figure 26: MTT analysis of A549 lung cancer cells treated with taxol.....	83
Figure 27: Histograms of flow cytometry data for A549 lung cancer cells.....	84
Table 10: Flow cytometric analysis of A549 lung cancer cells	85
Table 17: Mitotic indexes of control and taxol-treated A549 cells.....	86
VI. Discussion.....	87
VII. Future Directions	97
VII. Conclusion	98

List of Abbreviations

Appendix A: Buffers and Solutions

References

Acknowledgements

I would like to thank my supervisor, Dr. Zach Suntres, who made this project possible with his guidance and support. The freedom that he gave me to direct the project truly helped me to develop as a scientist. I also need to thank my other supervisors, Dr. Dimitrios Vergidis, who made himself available to listen to any problems and offered helpful suggestions, and Dr. John Th'ng - without his invaluable technical assistance I would not have been able to accomplish everything that I did. Thanks to my committee members, Dr. Law and Dr. Malek for their guidance and for editing this thesis.

I'd also like to thank the many other members of the lab who helped day-to-day and made coming to work fun. Specifically, Dr. Mary Lynn Tassotto and Rucy Vergidis for their guidance in all aspects of life, Lindsay Sutherland for being such a great ally in the lab, as well as a great TA partner and all-around great friend, and Michele Turner, Kyle Cullingham, Andy Cumming, Taylor Bureyko, Rebecca Barnes, Sean Gravelle, Sean Bryan, Chris Witiw, Marlon Hagerty, Pete Mitsopoulos, and the other students and techs for all the laughs and good times. Also, I would like to thank Dr. Amadeo Parrisenti and Dr. Marina Ulanova for providing me with the taxol-resistant MCF-7 cells and A 549 cells, respectively.

Last but not least, I have to thank my family and friends outside of the lab for their moral support throughout this whole process. My parents, brothers, Dave, Kerri, and the rest of my friends and family deserve credit for keeping me focused, giving advice, and listening to me practise my presentations.

Abstract

Taxol (paclitaxel) is one of the most effective chemotherapeutic agents used for the treatment of multiple cancers, including breast, ovarian, and, non-small-cell lung cancer. However, development of taxol resistance with prolonged use is common, requiring the use of the chemotherapeutic agent in combination with other treatments. In addition to the development of resistance, taxol is difficult to administer due to its high lipophilicity, and it requires solubilization with Cremophor EL (polyethoxylated castor oil) and ethanol, which often lead to adverse side-effects, including life-threatening anaphylaxis. Incorporation of taxol in DPPC:DMPG (dimyristoyl phosphatidylcholine: dimyristoyl phosphatidylglycerol) liposomes may not only eliminate the adverse reactions associated with the Cremophor EL vehicle, but also decrease other toxicities that arise from the drug's action in non-targeted tissues. Moreover, liposomally-encapsulated taxol might have the potential to overcome resistance by facilitating the cellular delivery of taxol at the site of action. Liposomes have been shown to be very effective in the delivery of other chemotherapeutic agents, such as adriamycin. This project deals with the use of liposomes as a novel delivery method for taxol. The effectiveness of liposomally-encapsulated taxol, as well as its ability to overcome taxol-resistance, was tested on MCF-7 breast cancer cells and A549 lung cancer cells. It was also tested for its ability to overcome taxol-resistance in two taxol-resistant MCF-7 cell lines. The results of our studies demonstrated the following: i) the lipid components of the liposomal formulation were non-toxic; ii) the liposomally-encapsulated taxol was more effective than conventional taxol in increasing the susceptibility of MCF-7 and taxol-resistant MCF-7 breast cancer cells as well as A549 lung cancer cells to taxol (as

determined by MTT cytotoxicity assays, DNA laddering, flow cytometry, and determination of mitotic indexes); and, iii) the improved effectiveness of taxol delivered as a liposomal formulation was associated with higher intracellular levels of the chemotherapeutic agent in cancer cells (determined by Ultra-Performance Liquid chromatographic technique). The results of these studies indicate that liposomes may be potentially used as a novel method for the delivery of taxol in cancer chemotherapy.

I. Introduction

Chapter 1: Chemotherapy and Paclitaxel

1.1 History of Paclitaxel:

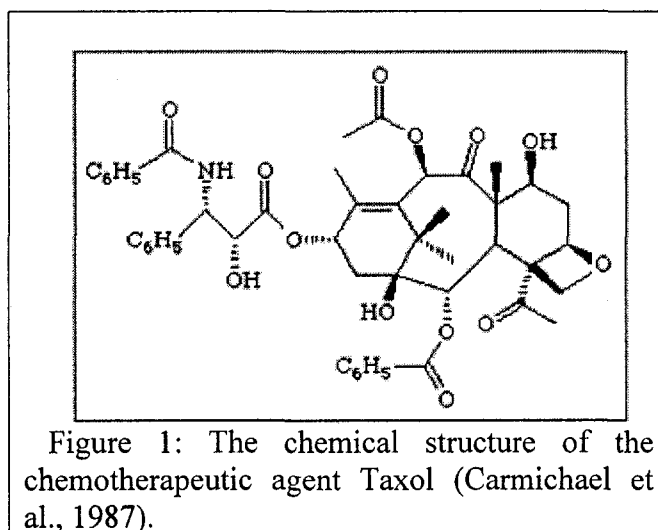
The original form of paclitaxel (taxol), derived from the Pacific yew tree (*Taxus brevifolia*), was discovered to exhibit marked anti-tumour activity against a variety of rodent tumours during a biological screening program initiated by the National Cancer Institute (NCI) in the early 1960's (Donehower, 1996). Although its biological activity was well-documented, little interest was shown in the compound until scientists at the Albert Einstein Medical College reported that it had a unique mode of action, at which point the NCI began clinical trials with paclitaxel in 1984 (Sengupta et al., 2001). However, isolation of taxol from the Pacific yew tree, a non-renewable resource, involved a slow and low-yielding process. As a result, the supply of yew trees, as well as taxol was quickly depleted (Donehower, 1996). In 1985, a diterpenoid comprising the complex tetracyclic core of paclitaxel called 10-deacetylbaccatin III (DAB) was isolated from the leaves of the European yew, which is a renewable resource. This discovery allowed the use of semisynthetic methods to secure a long-term supply of taxol (Miller et al., 2001). Because of the enormous cost of studying and manufacturing taxol, the NCI handed over the commercial rights to taxol to Bristol-Myers-Squibb (BMS) in 1989 (Cragg, 1999).

In December of 1992, the FDA approved taxol for the treatment of ovarian cancer, and in 1994 the drug was approved for the treatment of breast cancer. The process from initial isolation of the bark of the Pacific yew to the actual treatment of patients took

31 years. To date, taxol is the best-selling cancer drug ever manufactured, with its annual sales peaking in 2000 by reaching \$1.6 billion (Miller et al., 2001).

1.2 Chemical nature of Taxol:

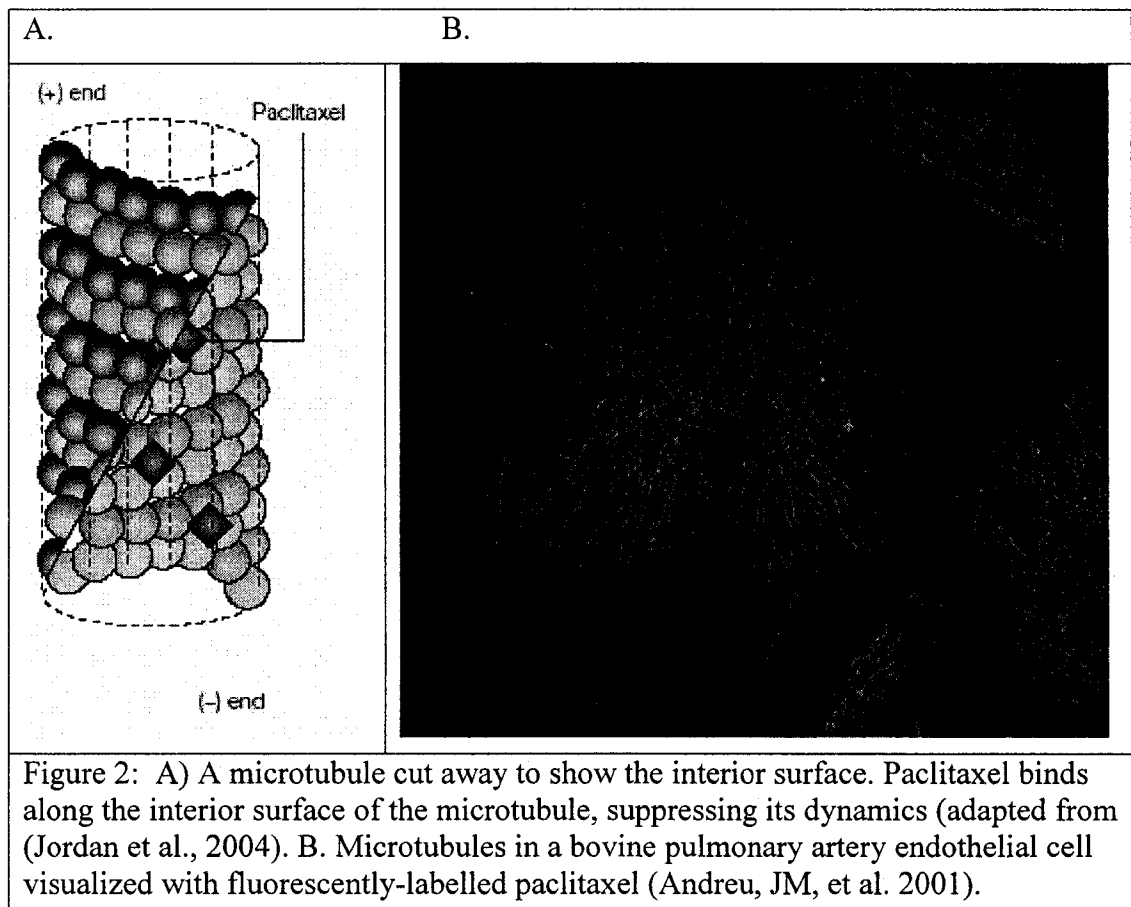
Taxol is a naturally-occurring poly-oxygenated diterpenoid with the chemical formula $C_{47}H_{51}NO_{14}$ and a molecular weight of 854.93 (Figure 1). Pure taxol is a white crystalline powder. It is insoluble in water, highly lipophilic, and it has a melting point of 217°C .



1.3 Mechanism of Action:

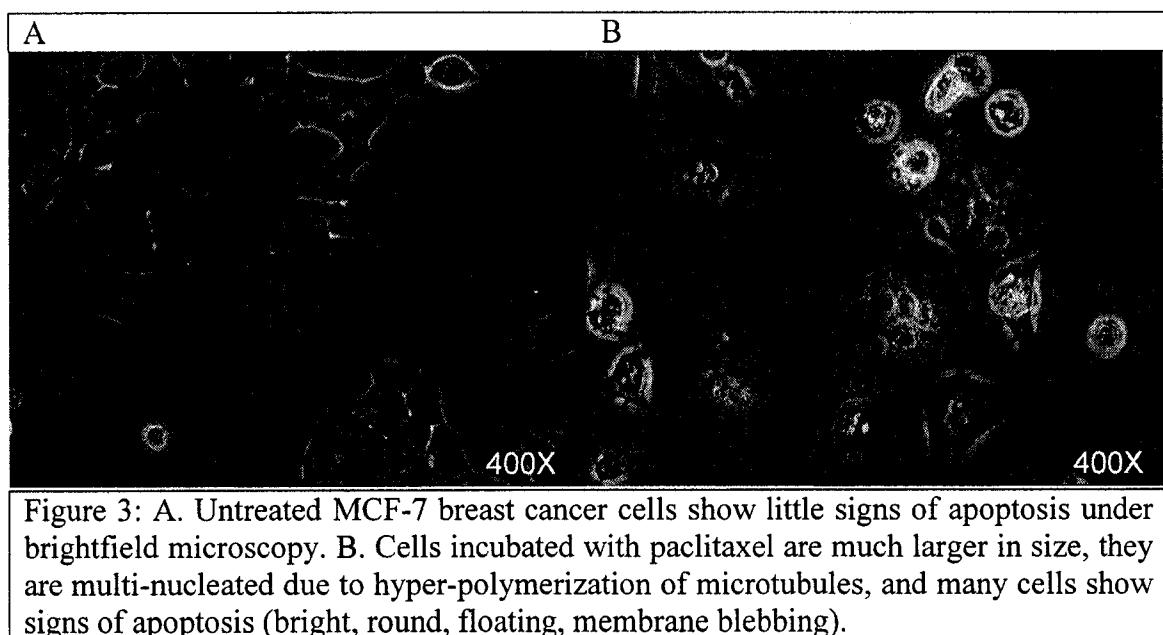
While other classes of chemotherapeutic drugs directly target DNA via its replication and regulatory proteins, paclitaxel interferes with the dynamic instability of microtubules. Specifically, it binds to the β -tubulin subunit of the tubulin protein that makes up microtubules to hyper-stabilize their structure (Figure 2). In normal cell

growth, these microtubules would be broken down or destroyed once the cell stops dividing, which is a process necessary for regular cell function. The ability to depolymerize microtubules via the removal of tubulin subunits also grants the cytoskeleton the flexibility needed for cellular transport. Once this flexibility is lost, chromosome movement is disrupted during mitosis, preventing further cell division by blocking the cell cycle in M phase, specifically between prophase and anaphase (Miller et al., 2001).



Following tubulin binding and M phase block, the cell enters cell stress, which involves the activation of specific pathways in the cell including MAP kinase activation

(Y. Huang et al., 1999). Under prolonged stress, the cell ultimately undergoes cell death or apoptosis (Figure 3). This mechanism affects both normal and cancerous cells, but since cancer cells are dividing at a much more rapid rate than non-cancerous cells, they are far more susceptible to paclitaxel-induced microtubule inhibition. Recent research has indicated that paclitaxel may also induce programmed cell death (apoptosis) in cancer cells by binding to an apoptosis stopping protein Bcl-2 (B-cell leukemia 2), thereby impeding its function (Michieli et al., 1999).



1.4 Pre-clinical Trials:

Prior to treatment of patients, any new drug must first pass a battery of tests examining its pharmacological activity and acute toxicity potential in humans. The overall goal of pre-clinical studies is to determine if the new treatment is reasonably safe for use in humans, and if it warrants further commercial development. Next, the creator

or sponsor of the drug must file a new drug application and begin a process of clinical trials that is both lengthy and expensive (Figure 4) (Hashida et al., 2005).

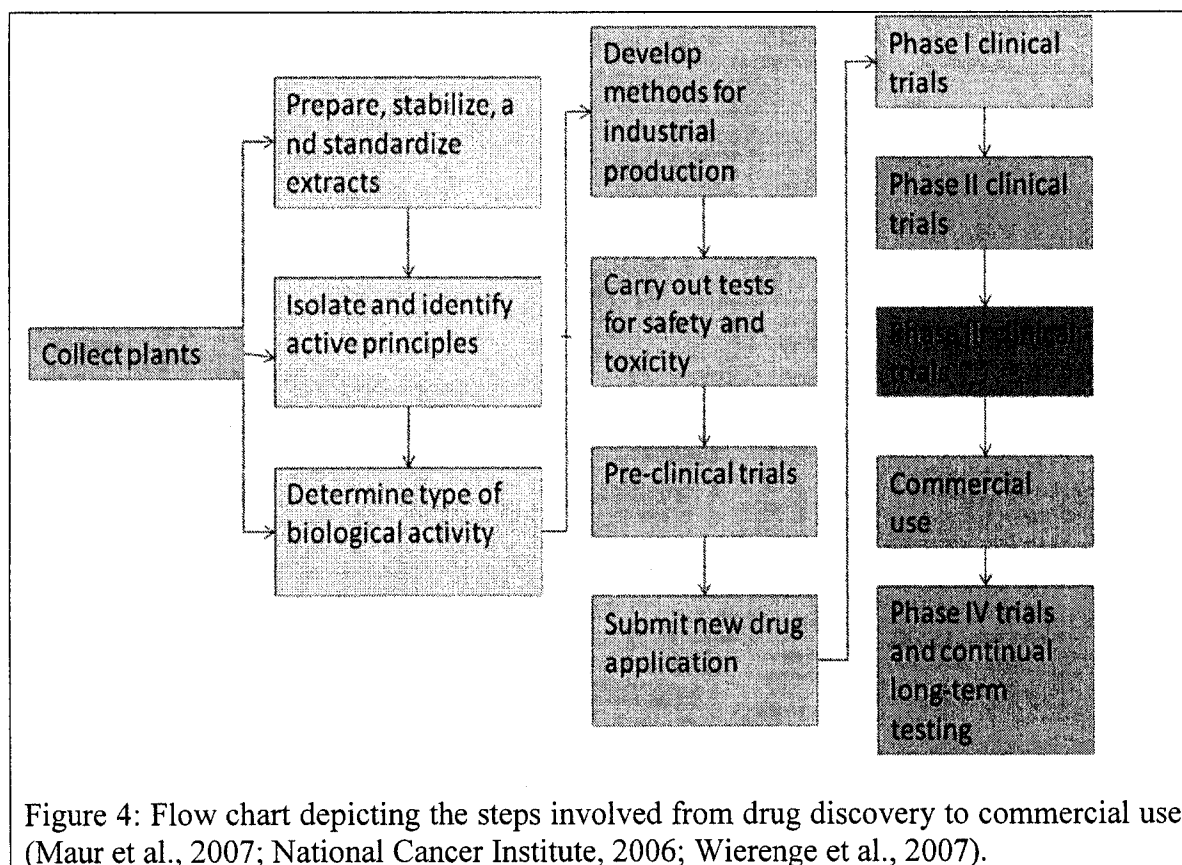
1.5 Clinical Trials:

Clinical trials are ethically-approved research studies carried out in order to improve the health care of patients by determining if promising approaches to cancer prevention, diagnosis, and treatment are safe and effective (National Cancer Institute, 2006). There are several different types of clinical trials, including trials for prevention, screening, diagnosis, treatment, and quality of life. It is one of the final stages of the drug discovery research process, and these trials can typically be broken down into three phases: phase I, phase II and phase III (Wierenge et al., 2007).

Phase I clinical trials involve a study on human subjects to determine how a new treatment should be administered, what dose should be given, and what side effects occur with increasing doses. These initial studies involve only a small number of subjects, and they may also determine the metabolism and pharmacologic actions of the treatment in humans. Phase I clinical trials for taxol began in 1984 and taxol was tested against a number of different cancer types (Cragg, 1999).

Phase II clinical trials are controlled clinical studies to determine the efficacy of the treatment for a particular indication. These studies are conducted with patients who have the disease in question, and they aim to determine any common side effects while continuing to test the safety of the treatment. In 1988, the results of Phase II trials testing taxol on ovarian cancer were extremely successful, which suggested the potential for the wide-spread use of the drug across the United States (Cragg, 1999).

Phase III clinical trials test a new treatment for a specific condition against the current standard treatment. These studies are only conducted if phase I and phase II studies indicate that the new treatment will be effective and safe. They gather additional information about the overall benefits and risks of the treatment, and they typically enroll a large number of patients. Following phase III clinical trials, a new treatment can be used for the general population, but it will continually be monitored for safety and to determine optimal use (National Cancer Institute, 2006). In 1989, it was announced that phase III trials of taxol on ovarian cancer were successful, and in 1991, it was determined that taxol was also effective for treatment of metastatic breast cancer (Cragg, 1999). Multiple phase III clinical trials are currently in progress testing taxol in combination with other chemotherapeutics and to determine its efficacy against different types of cancers.



1.6 Chemotherapeutic use in clinic:

Taxol is most commonly used to treat ovarian, breast, non-small-cell lung cancer, and AIDS-related Kaposi's sarcoma at a typical doses of 175 mg/m² (T. K. Yeh et al., 2005). Currently, clinical trials are being done to combine taxol with other anticancer drugs to treat many different types of cancer, such as lymphoma, and cancers of the stomach, esophagus, bladder, prostate, uterus, cervix, head, and neck. Taxol is useful over other chemotherapy treatments because of its unique method of action. Since taxol does not directly target the genome, it is effective alone as first-line treatment or in combination with DNA-damaging drugs in tumours that do not respond to other chemotherapies (Trock et al., 1997).

1.7 Current formulation of taxol:

Due to its low aqueous solubility (less than 0.03 mg/ml), paclitaxel is dissolved for clinical use in anhydrous ethanol and polyethoxylated castor oil (Chremophor EL) in a 1:1 (vol:vol) ratio. It is then mixed in a saline solution for delivery to the patient in a 1:10 (vol:vol) ratio, for a final concentration of 0.3 to 0.6 mg/ml. The primary elimination pathways for the Cremophor EL (CrEL) formulation of taxol involve hepatic metabolism and biliary excretion (Kennedy et al, 2004). CrEL is not an inert vehicle, and it has been shown to exert a range of biological effects. Specifically, CrEL has been shown to cause toxic side effects, including acute anaphylaxis (Gelderblom et al, 2001). The dose-limiting toxicity of taxol is neutropenia, which involves an abnormal decrease in the number of neutrophils (the most common type of white blood cells) in the blood. This condition is directly related to the duration of time that plasma taxol concentrations are at or above the threshold value (0.05 uM) (Kennedy et al., 2004). Other side effects include myelotoxicity, peripheral neuropathy, decreased bone marrow function, blood problems, liver damage, severe nausea and diarrhea, alopecia, and joint or muscle pain (Sparreboom et al., 2005; Trock et al., 1997). Antihistamines and glucocorticoids are administered to manage these adverse side effects, but despite this premedication, minor hypersensitivity reactions have been found in 41-44% of all patients, and major life-threatening reactions in 1.5-3% (Pakunlu et al., 2003).

In addition, these co-administered drugs have raised the possibility of additional pharmacokinetic and pharmacodynamic interactions with paclitaxel (Sparreboom et al., 1999). The CrEL vehicle also exerts a range of effects on the biodistribution of the drug, resulting in a nonlinear disposition (Sparreboom et al., 1999; van Tellinggen et al., 1999;

T. K. Yeh et al., 2005). Arterial paclitaxel has been shown to bind to fixed arterial elements, resulting in localization of the drug in proximity to the delivery source for some time after application. Such localization prevents efficient tumour targeting, thereby increasing the likelihood of side effects while decreasing efficacy (Giannakakou et al., 2000).

1.8 Recent Developments:

Recently, several research groups have attempted to develop alternative formulations of taxol in an attempt to avoid many of the problems associated with the Cremophor EL (CrEL) vehicle. ABI-007 (Abraxane) is a new formulation of taxol that does not use a solvent, but binds taxol to human albumin for delivery (Sparreboom et al., 2005). In a phase II study of this albumin-stabilized nanoparticle, advanced breast cancer patients had fewer side effects and responded well to the drug (Albumin-bound paclitaxel improves response rate vs docetaxel in metastatic breast cancer, 2007). In addition, premedication with steroids or antihistamines is not necessary with Abraxane, but is commonly administered with conventional taxol treatments (Green et al., 2006).

Chapter 2: Drug resistance

2.1 Models of drug resistance:

Current chemotherapy regimes involving paclitaxel (taxol) are not only limited by toxic side-effects, but also in part by the development of resistance, resulting in unnecessary and ineffective treatment and discomfort for the patient, as well as a waste of resources. Chemotherapy resistance is an important component of cancer mortality in current therapy regimes. There are two prevalent models of drug resistance: inherent (intrinsic) resistance, and drug-induced (acquired) resistance. Intrinsic resistance models predict an inherent resistance due to a change in gene expression, resulting in the activation of gene repair, activation of detoxifying systems, inhibition of drug influx, activation of drug efflux pumps, or blockage of apoptosis (Figure 5; Szakacs et al., 2006). In this model, the tumour shows no response to chemotherapy at the time of initial treatment. Alternatively, in the acquired resistance model, the tumour develops resistance after an initial response to treatment due to selection for drug-resistant cells in the tumour. It is expected that there is extensive overlap between the mechanisms responsible for these two distinct mechanisms of chemotherapy resistance (Morin, 2003).

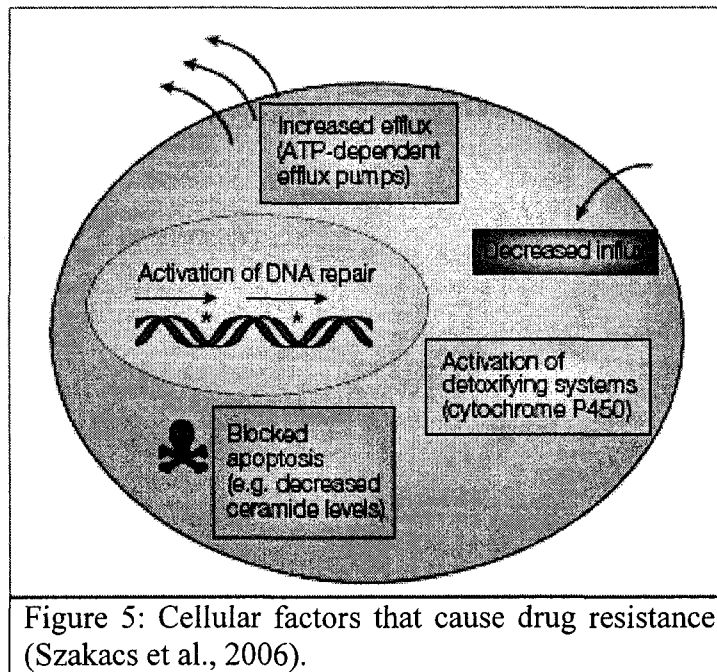


Figure 5: Cellular factors that cause drug resistance (Szakacs et al., 2006).

The acquired resistance phenotype is termed multidrug resistance (MDR), and it can involve resistance to numerous chemotherapies, such as the anthracyclines (doxorubicin, daunorubicin), the vinca alkaloids (vincristine), epipodophyllotoxins (etoposide), and taxanes (taxol, taxotere) (Yeh, et al., 2003). In drug-induced chemotherapy resistance, a process of successive rounds of selection and clonal expansion of resistant cells that express genes and proteins integral to drug resistance is the common model. In contrast, in intrinsic models of resistance, a fraction of tumours may already express such proteins without the selective pressure of chemotherapy treatment (Morin, 2003).

The principal molecules commonly implicated in either model of chemotherapy resistance include those involved in drug efflux, such as P-glycoprotein (MDR1) (Kamazawa et al., 2002), those involved in the apoptotic pathways, including Bcl-2, caspases, phosphatidylinositol 3'-kinase (PI-3) and downstream molecules (ex: AKT), genes involved in cell adhesion and cellular growth control, including peripheral myelin

protein 22 (PMP22) and integrin B5, and genes involved in DNA repair, such as BRCA1 (Lafarge et al., 2001).

2.2 Mechanisms of Taxol resistance:

Resistance to taxol can be modulated and enhanced by the Cremophor vehicle, which may induce an increase in expression of the P-glycoprotein (P-gp) efflux system by altering the disposition of the drug *in vivo* (Bhalla, 2003; Chiu et al., 2005). Class I P-glycoproteins have been shown to prevent the entry of paclitaxel across the blood-brain barrier, and to promote its excretion through the gut (Bhalla, 2003; Greiner et al., 1999) (Figure 6). This P-glycoprotein efflux pump is a member of the ATP-binding cassette (ABC) family of transporters, and it is encoded by the multi-drug resistance gene MDR1 (Gottesman, et al., 2002; Nakagawa et al., 1992). The MDR phenotype is one of the most widely accepted causes of chemotherapy failure in cancer patients. Of the 49 ABC transporter genes identified, ABCB1 (MDR1-P-gp) is one of the most well known, and it confers resistance to multiple chemotherapeutic agents by exporting taxol and other cytotoxic, hydrophobic drugs from inside the cell to the extracellular space (Kamazawa et al., 2002; Yeh et al., 2003). These ABC transporters regularly function to detoxify and protect the body from xenobiotics, and they are often highly expressed in important pharmacological barriers (Gottesman et al., 2002; Greiner et al., 1999).

Through the acquisition of the MDR phenotype, it has been surmised that tumour cells actively reorganize their microenvironment to increase cell adhesion and drug resistance. Specifically, the tumour cells themselves may produce a favourable extra-

cellular matrix (ECM) by conditioning the neighbouring stroma to induce the production of proteins such as collagen V1 and E-cadherin (Morin, 2003).

Gene expression profiling studies have shown MDR1 and its family members to have a multiple-fold increase in expression levels in taxol-resistant cell lines (Sugimura et al., 2004; Trock et al., 1997; Villeneuve et al., 2006). These data support the role of ABC transporters in drug resistance, but they also indicate a much more complex system with no universal set of resistance genes.

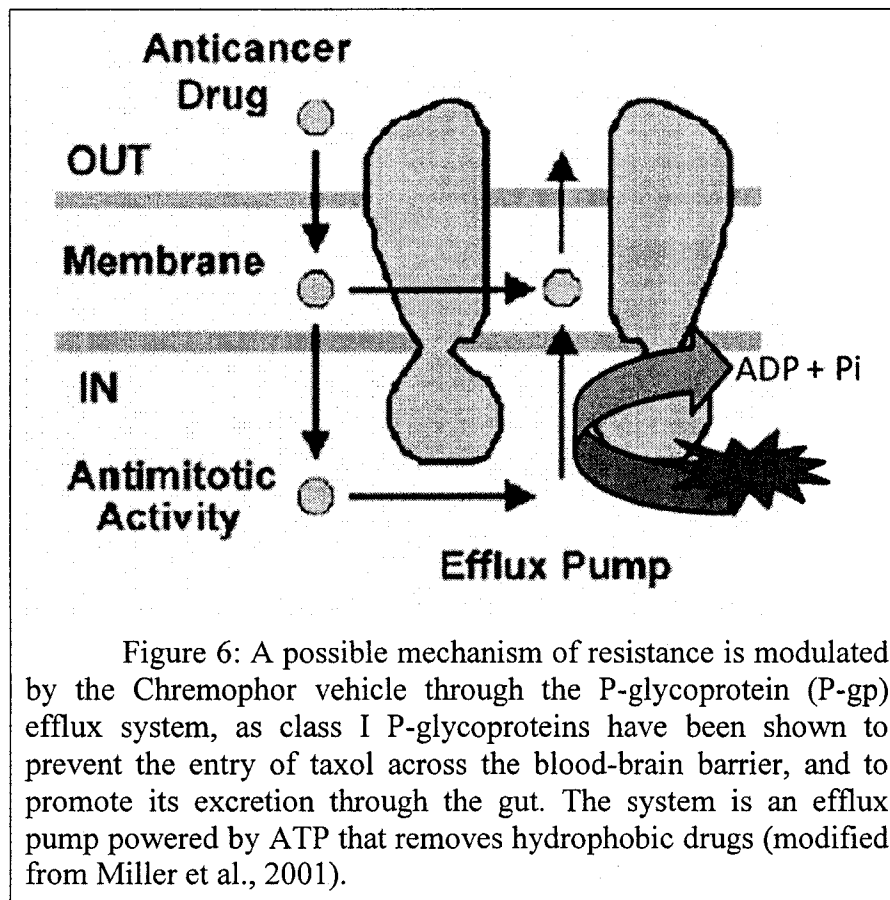


Figure 6: A possible mechanism of resistance is modulated by the Chremophor vehicle through the P-glycoprotein (P-gp) efflux system, as class I P-glycoproteins have been shown to prevent the entry of taxol across the blood-brain barrier, and to promote its excretion through the gut. The system is an efflux pump powered by ATP that removes hydrophobic drugs (modified from Miller et al., 2001).

Another potential mechanism of intrinsic paclitaxel resistance is the presence of beta-tubulin point mutations in tumour genomic DNA. Such mutations may impair the ability of paclitaxel or GTP to bind to the tubulin, thereby conferring resistance to the drug (Massing et al., 2000; Michieli et al., 1999; Monzo et al., 1999; Theodoulou et al., 2004). In addition to these, class III beta-tubulin (β -tubulin) over-expression may also play a key role in the development of drug resistance (Ferlini et al., 2003; Mross et al., 2004). *In vitro* studies of paclitaxel resistance have shown that overexpression of class III β -tubulin induces paclitaxel resistance by reducing the ability of paclitaxel to suppress microtubule dynamics (Kavanagh et al., 2005). Mutations in β -tubulin confer resistance to taxol by altering microtubule dynamics, and not by interfering with the binding of taxol to microtubules (Bhalla, 2003). The different tubulin isotype classes vary in their paclitaxel binding affinities, and type III β -tubulin has been identified at higher concentrations in tumour cell lines that are resistant to paclitaxel. These increased β III-tubulin levels may be attributed to the expression of oncogenic epidermal growth factor receptor (EGFR) family kinases (Montgomery et al., 2000).

Alternatively, Bcl-2 phosphorylation is a known marker for mitotic arrest and can be induced by paclitaxel in cellular systems. It has also been shown to be the earliest detectable molecular event linking microtubule disruption to apoptosis (Moos et al., 1998). *In vitro* studies have also shown that paclitaxel resistance can be introduced through the inducible expression of the anti-apoptotic Bcl-2 family member, Bcl-xl via paclitaxel treatment. These results suggest a role for paclitaxel in the mediation of the expression of this family of proteins, resulting in resistance to the drug. Another study of gene signatures of paclitaxel resistance found that taxol-resistant breast cancer cells were

found to possess markedly higher levels Bcl-2 compared to a wild-type parental cell line (Villeneuve et al., 2006). Members of the Bcl-2 family, including Bcl-xl are also commonly overexpressed in primary tumour samples, and have primarily been associated with chemoresistance and shorter disease-free survival (Williams et al., 2005).

Whatever the mechanism, drug resistance conferred or modulated by CrEL can pose a great problem in patient care. With all of the problems associated with the current vehicle, alternate pharmaceutical strategies must be explored to achieve optimal chemotherapeutic results using taxol. Encapsulation of chemotherapy agents into nanoparticles such as liposomes has proven to be an effective strategy with great potential to overcome resistance and alleviate some of the toxic side effects associated with conventional therapies (Hofheinz, et al., 2005; Massing et al., 2000; Sengupta et al., 2001; Theodoulou et al., 2004).

2.3 Measuring Drug resistance and apoptosis:

The technique often employed in studying acquired drug resistance involves identifying chemotherapy-resistant cellular models and conducting gene or protein expression assays comparing the resistant cells to their sensitive counterparts. More recent work has focused on the use of patient samples and microarray technology to determine global gene expression, and to monitor the change in expression as resistance forms with treatment (Lamendola et al., 2003; Lee et al., 2004).

Due to the fact that there are no proven predictors of a patient's response to chemotherapy, all cancer patients selected for chemotherapy will receive the same treatment regime, regardless of their genetic background or any other individual factor.

Individualized treatments are not currently used to treat patients based on their susceptibility or resistance to any particular drug. This can be attributed, in part, to the fact that no universally accepted guidelines for complete analytical or clinical validation of anticancer resistance exist. As a result, differences in techniques such as tissue collection methodologies, molecular targets, apoptosis assays, or variations of protocols have limited the ability to compare various studies from different institutions. In addition, there is an absence of standardized criteria to score the immunohistochemistry staining for chemoresistant protein expression, leading to observer bias, and making it difficult to compare results between different researchers. These factors all limit the ability of clinical trials to validate work done *in vitro*.

The World Health Organization (WHO) and more recent Response Evaluation Criteria in Solid Tumours (RECIST) criteria for clinical tumour response evaluation are simple to use and they are widely accepted as a measure of the therapeutic effect of anticancer agents. They were designed to allow for international standardization of the reporting of cancer treatment results, and they classify treatment outcomes into four categories based on measurements of tumour size over time. The response to therapy can be classified as a complete response, partial response, no change, or progressive disease (Padhani et al., 2000). These two sets of guidelines are comparable, with the main difference being in the method of measurement; the newer RECIST guidelines use unidimensional rather than bidimensional measurements of tumour diameter, meaning that RECIST criteria utilize the sum of the longest diameters of tumours, rather than the bidimensional WHO method, which uses the product of the longest diameter and that perpendicular to it, summed over all tumors (Gehan et al., 2000; Park et al., 2003).

However, the WHO and RECIST criteria do not provide specific instructions on the methodology of performing tumour measurements, and as a result, discrepancies due to interobserver and intraobserver variability still exist in many cases, even when following the WHO and RECIST guidelines (Erasmus et al., 2003). Such inconsistencies often arise from observer variations in the identification and position of lesion boundaries, which can be difficult or nearly impossible to measure. In addition, measurement errors that estimate the size of small lesions can often result in the misclassification of tumour response. Furthermore, variations in examination technique between independent review panels can account for disagreements in tumour size, and ultimately, tumour classification (Padhani et al., 2000).

With phase I and II clinical trials often being performed on a small group of patients, the outcome may be impacted by even the smallest differences in reported tumour size, making any inconsistencies particularly problematic. As a result, clinical response as determined by RECIST or WHO must be evaluated in combination with other clinical factors, such as time to progression, disease-free survival (DFS), and overall survival (OS) in order to determine an actual survival benefit for a particular therapeutic agent (Padhani et al., 2000). In addition, the biochemical measure of antitumour effect in patients can provide another method to confirm tumour measurements.

Molecular markers studied in the laboratory are more reflective of biological response, which may be assessed before actual clinical response is detectable. However, much more work will be necessary to determine the actual predictive value of biological response with respect to clinical benefit. Research groups have formed in order to create

guidelines for performing specific studies, such as the RITA-CEPA group, which has standardized the assessment of cell proliferation studies using bromodeoxyuracil (BRDU) incorporation. Their guide includes organ-specific photo guides to define staining thresholds and intensities, as well as methods to analyze generated data, and their aim is to provide standardization in order to increase the value of data obtained and the conclusions drawn (Nolte et al., 2005). For specific and specialized studies it may be possible to standardize protocols, but for many other techniques, there is a great variance in laboratory practise between various institutions.

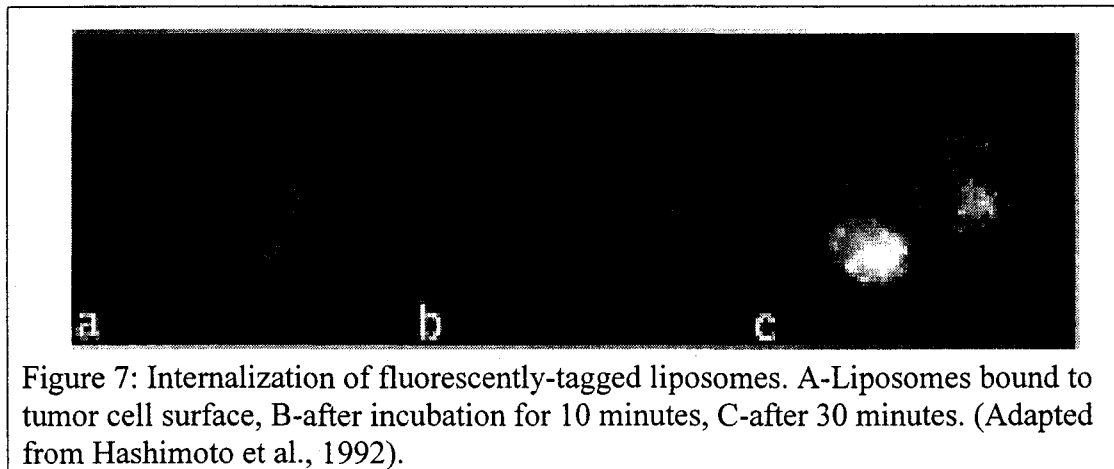
2.4 Strategies to overcome resistance:

There are numerous methods that have been employed in an attempt to overcome drug resistance both *in vitro* and in the clinical setting. Many focus on the encapsulation of chemotherapy drugs into liposomes, microspheres, or nanoparticles that would ideally escape the common mechanism of resistance, namely the p-glycoprotein efflux pump. Alternatively, oligo-nucleotides that are antisense to resistance genes (ie: MDR1, Bcl2, etc), have been used in gene therapy *in vitro* in an attempt to block the function of these genes in the cell and overcome resistance (Pakunlu et al., 2003). Water-soluble copolymer prodrug administration has also been investigated as a potential mechanism to overcome resistance (Zou, et al., 2004). However, these methods have not all been employed in combination with taxol, leaving many avenues of research for further study in increasing the effectiveness of taxol in chemotherapy regimes.

Chapter 3: Liposomes

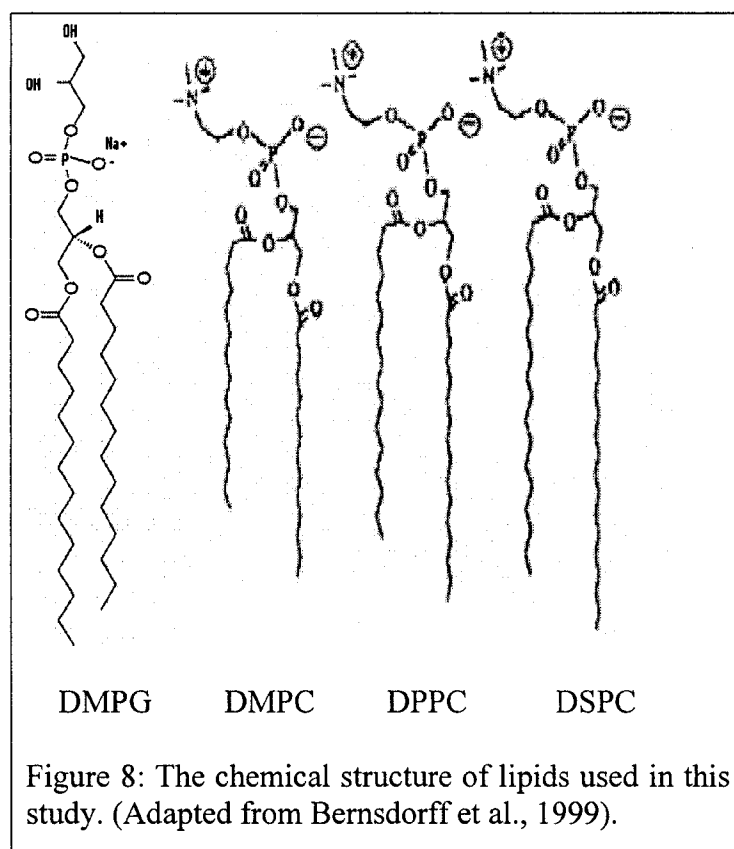
3.1 Liposomes:

The word “liposome” comes from the Greek words “lipid,” meaning “fat”, and “soma,” meaning “body”. Liposomes are lyotropic liquid crystals, meaning that the ordering effects of the lipids are induced by changing the concentration within a solvent. They form self-assembling vesicles with an inner aqueous compartment surrounded by a lipid bilayer of naturally-occurring phospholipids (Goyal et al., 2005). They have a low intrinsic toxicity, and they are non-immunogenic, biocompatible, and biodegradable. Both lipophilic and hydrophilic drug types can be incorporated into liposomes; lipophilic drugs can be integrated into the phospholipid bilayer, while hydrophilic drugs can be stored in the inner aqueous compartment. To deliver liposomes to the site of action, the liposome’s phospholipid bilayer can fuse with other bilayers such as the cell membrane, thus delivering the contents. As a result, particles or drugs that would not normally be able to diffuse through the membrane can be indiscriminately delivered past this bilayer. Alternatively, if liposomes are small enough in diameter, they may be taken up directly by the cell through endocytosis (Figure 7; Hashimoto et al, 1992).



3.2 Structure and composition of liposomes:

The specific composition of liposomes can differ, as several possible formulations using various phospholipids or surfactants, in varying ratios, will be used to successfully incorporate taxol within them. The use of naturally-occurring phospholipids is important for drug delivery in order to abrogate any immunogenic response within the body. The surfactants dimyristoyl-phosphatidyl-glycerol (DMPG), dimyristoyl-phosphatidylcholine (DMPC), dipalmitoyl-phosphatidylcholine (DPPC), and disaturated-phosphatidylcholine (DSPC) can be produced synthetically, but are naturally-occurring (Figure 8; Bernsdorff et al., 1999). They are the main components of natural human lung surfactant, and DPPC accounts for 60-70% by weight in normal humans. Lung surfactants are a mixture of lipids and proteins that coat the inside of mammalian lungs. They function to reduce the work of breathing by forming a monolayer at the alveolar air/water interface, making them capable of lowering surface tension to near zero values. These surfactants can be used in combination to determine an optimum formulation for the efficient encapsulation and retention of paclitaxel for delivery to cells.



Another feature of liposomes is their versatility. In addition to the numerous types of potential lipid components, liposomes can be coated in a polyethylene glycol (PEG) layer, which is inert in the body, allowing the liposome to have a longer circulating time in the blood. Liposomes with this coating are referred to as “stealth liposomes,” as PEG aids in the circumvention of macrophages of the immune system that are found in the blood stream, which primarily occurs in the liver or spleen (Vyas, et al., 2006). Pegylation functions to create a large hydrodynamic volume, thereby increasing the molecular mass of the peptides (Molineux, 2002). This increased volume helps to shield the proteins from proteolytic enzymes (Harris et al., 2003; Yowell et al., 2002). Further, specific vitamins, antigens, or antibodies can be attached to the phospholipid bilayer in order to target a specific tumour type (Goyal et al., 2005) (see below).

3.3 Targeting liposomes:

There are numerous methods utilized to target liposomes to a specific cell type, including noncovalent association of cell specific antibodies, coating with heat aggregated immunoglobulins M (IgM), addition of glycoproteins or glycolipids, or covalent attachment of poly and monoclonal antibodies to the liposomes, which are then called “immunoliposomes” (Goyal et al., 2005). These immunoliposomes are potent carriers that result in the acceleration of cellular uptake due to the recognition of the antibody by the target cell (Hatakeyama et al., 2007). Immunoliposomes have been created to target multiple components of cancer cells, including membrane type 1 matrix metalloproteinase (MT1-MMP) (Atobe et al., 2007; Hatakeyama et al., 2007), surface-bound nucleosomes (Elbayoumi et al., 2007), and Bcl-2/Bcl-x1 (Hussain, et al., 2006), among others.

3.4 The Enhanced Permeability and Retention effect:

The endothelial wall of normal human blood vessels is typically encapsulated by endothelial cells that are bound together by tight junctions, which function to maintain structure and to stop any large particles in the blood from leaking out of the vessel. Liposomes up to a diameter of 400-600 nm are able to accumulate in tumour tissue in a passive yet selective fashion due to an increased “leakiness” of tumour vasculature (Hashida et al., 2005). This is known as the enhanced permeability and retention effect (EPR effect), and it is reinforced by the accelerated growth of blood vessels in tumours. As a result, cancerous tissues are more likely to take up liposomes, while healthy tissues with regular growth rates are less likely to do so. In addition to this enhanced

permeability effect, the cells that make up tumours are often spaced further apart, allowing accumulation and retention of liposomes in this intercellular space. Also, the lymphatic system that typically removes nanoparticles like liposomes from healthy tissues is often only marginally found in tumour tissues, which facilitates the retention of liposomes in the targeted tumour tissue (Hofheinz et al., 2005).

3.5 Liposomal encapsulation of anticancer agents:

Encapsulation efficiency is determined by the composition of the liposome, including the lipid content used and the particle size. Encapsulation efficiency must be balanced with substrate permeability to achieve a useful formulation for drug administration. In addition, the liposomes must be able to retain paclitaxel long enough to use them for effective clinical administration.

Encapsulation of anti-cancer drugs into liposomes has been shown to result in their accumulation to higher concentrations in the tumour interstitium than following conventional delivery, as the potentially troubling pharmacokinetics of the drug are replaced by the pharmacokinetics of the liposomes (Chiu et al., 2005). As a result, the level of plasma clearance and the volume of distribution are reduced. Overall, the therapeutic index of the drug is improved, while the side effects of the drug can be reduced, or in some cases, eliminated (Duan et al., 2004; Tzafiriri et al., 2005; Yeh et al., 2005).

For example, liposomal doxorubicin has been shown to reduce the cardiotoxicity that is often associated with its conventional delivery method (Tzafiriri et al., 2005). As a result, the lifetime cumulative dose potential for doxorubicin treatment is increased with

the liposomal formulation. This is a limiting factor in the current conventional therapy (Theodoulou et al., 2004). Two formulations of liposomal doxorubicin are currently used in clinic to treat patients. Caelyx® is used to treat Kaposi's sarcoma, and advanced recurrent ovarian cancer, and Myocet® is used to treat advanced metastatic breast cancer (Mross et al., 2004). In addition to alleviating side effects, these liposomal formulations have been shown to result in a longer half-life of the drug, and an increased therapeutic index (Colombo et al., 2007; Mross et al., 2004).

Similar results have been found with liposomal etoposide, where myelosuppression was inhibited while the maximum tolerated dose was increased (Soepenberg et al., 2004). Liposomal daunorubicin was found to be more toxic than the free drug against multi-drug resistant cells, suggesting that liposome encapsulation can partially protect the drug from the P-glycoprotein efflux system (Massing et al., 2000). These studies demonstrate great potential for effective therapy using liposomal encapsulation of anticancer drugs.

3.6 Other liposomal treatments:

Liposomal drug delivery has proven to be a successful mode of treatment in cancer therapy as well as in the delivery of other forms of therapy, such as treatment involving metal chelation, vaccine, enzyme and hormone replacements, diagnostic imaging, and the treatment of skin and eye diseases, among others (Goyal et al., 2005). Aside from cancer treatment, liposomes have had the most success in their use as a vehicle for antimicrobial and antiviral treatment (Goyal et al., 2005).

Several types of antimicrobial drugs have been incorporated into liposomes, including those used to treat mycobacterial infections, fungal infections, and

mycobacterial infections. In order to be effective in the treatment of mycobacterial infections, drugs must be able to effectively penetrate the host macrophage, infect intracellular sites, and preferably have reduced toxicity with ample effect at low doses to allow prolonged therapy (Goyal et al., 2005). Furthermore, antibiotics are only effective against intracellular infections if they can penetrate phagocytic cells. Liposomes provide a useful mode of delivery because they are able to localize in the liver and spleen, where many pathogenic microorganisms reside, and they can increase intracellular targeting in these cells (Goyal et al., 2005).

Liposomes are also effective for delivery of antiviral therapy due to their ability to deliver the encapsulated drug across the cell membranes to and this effectively concentrates them at the disease site (Sinico et al., 2005). Specifically, liposomes have been used to treat herpes, hepatitis C and HIV (Ferguson et al., 2006; Pecheur et al., 2007; Sinico et al., 2005). In addition to chemical drugs, liposomes have been used as a delivery method for oligonucleotide agents and small interfering RNAs (siRNAs) which can be used to induce expression of certain proteins or knock-down gene expression in a sequence-specific manner (Hussain et al., 2006).

Liposomal delivery of gene therapy has been a popular avenue of investigation as liposomal encapsulation protects these agents from degradation by cellular enzymes (Ferguson et al., 2006; Schyth et al., 2007). In addition, liposomes allow transfection of large-sized genetic material to the cell in comparison to the conventional use of viral transfection methods. Furthermore, liposomes are a safer method of delivery, as the risk of the virus becoming replication-competent and infectious is always a possibility (Goyal et al., 2005). Liposomes have not widely been used in gene therapy as a viable

alternative to viral vectors as of yet, but it represents an avenue of research that is currently under investigation for numerous applications.

3.7 Liposomal taxol:

Several attempts have been made to replace Cremophor EL as a vehicle for the delivery of taxol by incorporating it into liposomes. However, due to the insoluble nature of taxol, problems involving entrapment efficiency and stability are often encountered. One group encountered difficulties when attempting to achieve acceptable entrapment efficiencies (Ceruti et al., 2000). As a result, water-soluble prodrugs of taxol were incorporated to increase the efficiency, yet no difference in cytotoxicity was detected between the liposomal and conventional taxol formulations. However, PEG-ylated liposomes were shown to increase plasma half-life (Ceruti et al., 2000; Crosasso et al., 2000). Another group attempted to increase stability by introducing cationic lipids, which differ from the usual neutral or anionic compositions. This method increased stability, but was not tested for efficacy (Campbell et al., 2001). In one case, a phase I study of a liposome-encapsulated taxol formulation was conducted, but the trial was discontinued, as the liposomal formulation showed no improvement over current taxanes in use (Soepenbergh et al., 2004).

II. Summary

Taxol is a powerful chemotherapeutic agent with a unique method of action that is primarily used to treat breast, ovarian, and non-small-cell lung cancers. However, it is difficult to administer due to its high lipophilicity, and as a result, it is dissolved in Cremophor EL, which has been associated with multiple adverse side effects, including life-threatening anaphylaxis. In addition, this vehicle is known to modulate the common development of drug resistance with prolonged treatment.

Drug resistance can be acquired or intrinsic, and multiple pathways have been implicated in taxol resistance, including expression of the protein membrane pump P-glycoprotein, phosphorylation of the Bcl-2 family of proteins, mutations in the B-tubulin subunit of microtubules, and overexpression of the class III B-tubulin subtype, among others. Many studies have been conducted in an attempt to better understand these pathways and to develop methods to overcome drug resistance.

Liposomes are composed of naturally-occurring phospholipids that are self-assembling with an inner aqueous compartment surrounded by an outer lipid membrane layer. Both lipophilic and hydrophilic drugs can be incorporated into liposomes for drug delivery. Due to enhanced permeability and retention (EPR) effect, liposomes are known to preferentially accumulate in tumour tissues, making them particularly suitable for delivery of chemotherapeutics. Current liposomal drugs, such as liposomal doxorubicin have been shown to improve the therapeutic index, while alleviating the toxic side effects of the drug. Liposomal encapsulation of taxol intends to assuage the common side effects associated with its use, while circumventing the development of resistance to the drug.

III. Objectives

Objective 1: Develop and characterize a paclitaxel-resistant breast cancer cell line. The chemotherapeutic effectiveness of paclitaxel will be evaluated in a breast cancer cell line (MCF-7) and two paclitaxel-resistant cell lines (clone and tax-resistant), which were established from the cancer cell line MCF-7 via successive selections of surviving colonies after paclitaxel treatments. These cell lines will be characterized for expression of the P-glycoprotein efflux pump and used to determine whether delivery of paclitaxel as a liposomal formulation escapes the efflux by this pump.

Objective 2: Develop and characterize formulations of liposomal paclitaxel. The liposomal formulations will consist of phosphatidylcholine (DMPC; DPPC; DSPC) and phosphatidylglycerol (DMPG). The choice of liposomal paclitaxel formulation that will be used in the subsequent experiments will be determined following characterization of the liposomal formulations for size (by particle size analysis), encapsulation efficiency, and stability.

Objective 3: Evaluate and compare the *in vitro* chemotherapeutic effectiveness of paclitaxel delivered to cultured breast cancer cells as a liposomal or conventional formulation. Flow cytometric analysis of the cell cycle will be used to compare the effectiveness of both the conventional and liposomal formulations of paclitaxel after treatment of cell cultures, and to determine the type of cell death that follows. The MTT cytotoxicity assay, mitotic indexes and DNA laddering will be used to assess the extent of cell injury. Ultra-performance liquid chromatography (UPLC) will be used to analyze the cellular uptake of taxol by cultured cells challenged with the different paclitaxel

formulations and assess whether the extent of injury is directly related to the intracellular concentration of paclitaxel.

V. Materials and Methods:

Part 1: Establishment of a taxol-resistant MCF-7 clone

4.1 Propagation of cultured cell lines:

MCF-7 cells are epithelial adenocarcinoma cells derived from a pleural effusion metastasis from a primary tumour in the mammary gland of a 69-year-old female. They were maintained in Dulbecco's Modified Eagle's Medium (DMEM; Hyclone) supplemented with 10% (v/v) fetal bovine serum (FBS), 100 µg/ml penicillin, and 100 µg/ml streptomycin in a 5% (v/v) CO₂ atmosphere at 37°C. MCF-7 cells were obtained from the American Tissue Culture Collection (ATCC). These MCF-7 cells (termed "wild-type A") were used to create a taxol-resistant colony (termed "clone"). Normal MCF-7 cells (termed "wild-type B") and a taxol-resistant cell line, (termed "tax-resistant"), were also generously donated for this study by Dr. A. Parissenti from the Northern Ontario School of Medicine (East campus).

A549 cells are epithelial cells (donated by Dr. Marina Ulanova) initiated through explant culture of cancerous lung tissue from a 58-year-old Caucasian male. They were maintained in DMEM/Ham's F12K medium (Hyclone) with L-glutamine and additionally supplemented and maintained as detailed above.

Human dermal fibroblast cells (HSF-55) are derived from human skin. They are not transformed, and therefore they have a limited lifespan. These cells were used to determine the effects and toxicity of treatment with liposomes on non-cancerous tissue. They were maintained in similar culture conditions as the MCF-7 cells, as detailed above. HSF-55 cells were generously donated by Dr. M. Tassotto at the cancer research lab in

the Thunder Bay Regional Health Sciences Center. A summary of the cell lines used in this study is given in Table 1.

Table 1. A summary of cell lines used in this study			
Cell line	Type of cells	Abbreviation	Source
MCF-7	Breast cancer	Wild-type A	ATCC
MCF-7	Breast cancer	Wild-type B	Dr. A. Parissenti
MCF-7 (taxol-resistant)	Breast cancer	Clone	Isolated for this study from wild-type A
MCF-7 (taxol-resistant)	Breast cancer	Tax-resistant	Dr. A. Parissenti
A549	Lung cancer	A549	Dr. M. Ulanova
HSF-55	Skin	HSF-55	Dr. M. Tassotto

4.2 Treatment of Cells

Unless otherwise indicated, cell cultures were plated, left overnight to adhere, and additional media containing serial dilutions of the treatment were added the following day. Cells in treatment were incubated in 5% (v/v) CO₂ atmosphere at 37°C between 24 hours and 7 days, depending on the assay. The taxol used for encapsulation into liposomes was pure taxol in powder form, and “conventional taxol” in the Cremophor vehicle was purchased from Bristol-Myers Squibb (BMS) and donated by the pharmacy in the Cancer Centre of the Thunder Bay Regional Health Science Centre.

4.3 Doubling time analysis:

For each cell line, twenty-thousand cells were plated in each well of two 6-well dishes. Cells were allowed to adhere overnight. The next day, one well of each plate was trypsinized and the cells were counted five times using an automated cell counter

(Beckman Coulter). The counts for the two wells were averaged. Every second day, two more wells were trypsinized and counted in a similar manner. The equation of the trendline of best fit was determined using Excel, and doubling time was calculated from this equation using the following formula [equation (1)]:

$$(1): [\text{LN}(\text{Time2}/\text{slope})/\text{exponent}] - [\text{LN}(\text{Time1}/\text{slope})/\text{exponent}],$$

Cell doubling times were used to characterize resistant cell lines and their parental counterparts, as well as to determine the length of cell cycles for treatment of the various cell lines with taxol.

4.4 Establishing an MCF-7 taxol-resistant cell line (clone):

MCF-7 cells were obtained from the American Tissue Culture Collection. Cells were split into three 150 mm plates at a concentration of 2.1×10^5 cells per plate and taxol was added to each plate for a final concentration of either 1 μM , 7.5 μM or 15 μM . After four days, plates were rinsed with 1X PBS to remove dead floating cells, and fresh medium was added with the same concentrations of taxol. Cells were rinsed with PBS and medium was replaced two times over the following 12 days, and after 16 consecutive days of taxol treatment, cells from the 1 μM and 7.5 μM plates were trypsinized and split into two 100 mm culture dishes, leaving two plates from each drug treatment group. (No living cells were left after 15 μM treatment). One plate from each treatment group was left in fresh medium without any taxol, and the other plates were treated with 0.1 μM taxol. Cells in 100 mm culture dishes were maintained once per week for approximately 45 days, at which point distinct colonies were visible on the plates cultured in medium without drug. Twenty-four colonies were selected and moved into individual wells of a

12-well plate and allowed to adhere overnight. After 24 hours, colonies were trypsinized and split into two identical replicate plates to re-disperse the cells within the wells. Re-dispersed cells were allowed to adhere overnight, at which point the replicate wells were treated with either 1 μM or 2 μM taxol to check for resistance. A summary of this process is shown in Figure 9. Six clones with favourable growth characteristics under taxol treatment were selected to undergo a colonization assay.

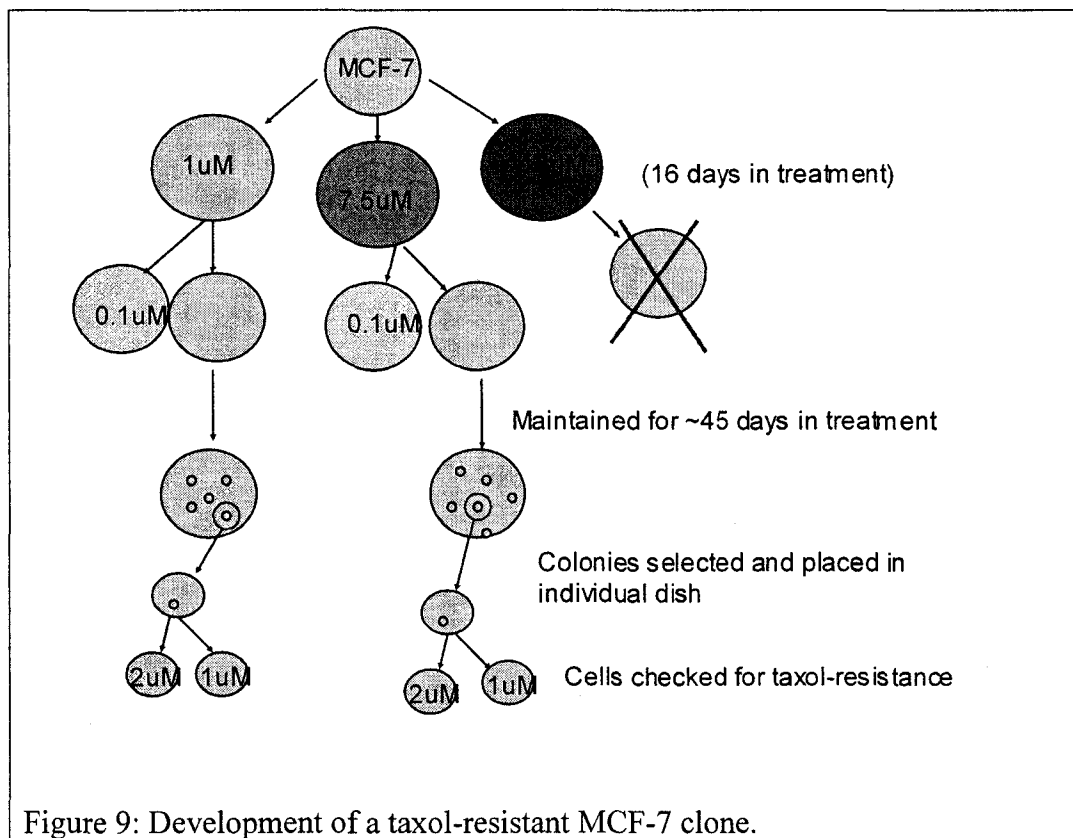
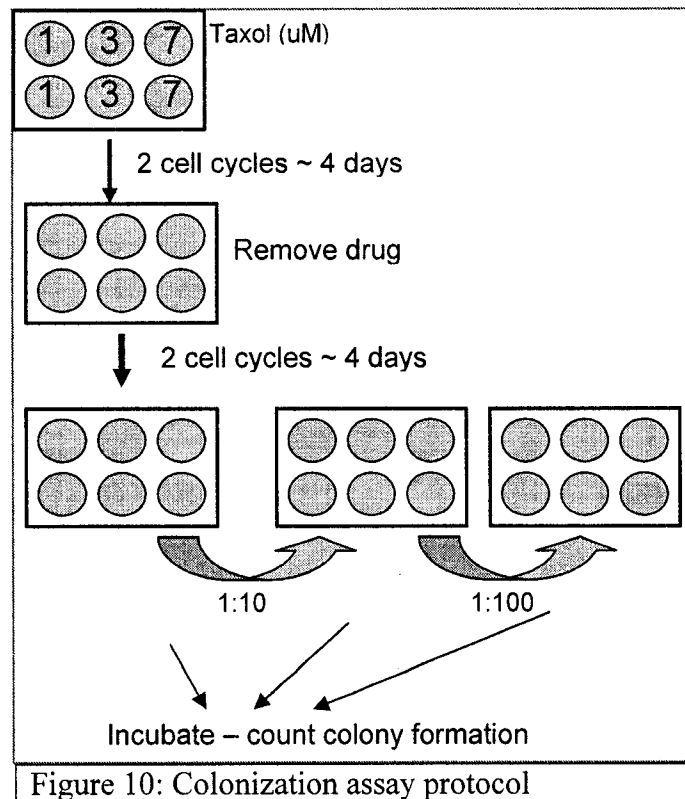


Figure 9: Development of a taxol-resistant MCF-7 clone.

4.5 Colony formation assay:

To characterize and compare resistant clones isolated from successive taxol treatments, a colony formation assay was performed. This experiment was also used to

determine if cells treated with various doses of taxol could eventually resume growth to form colonies or whether they were destined for apoptosis. Six colonies of potentially taxol-resistant MCF-7 clone cells were plated in 6-well dishes and treated with serial dilutions of taxol for 2 cell cycles (as determined by doubling time analysis – section 4.3). These were compared to parental MCF-7 cells (wild-type A), as well as another MCF-7 cell line (wild-type B) and a taxol-resistant cell line (Tax-resistant). After treatment, the drug was removed and replaced with fresh medium for an additional 2 cell cycles. Cells were then trypsinized and plated in serial dilutions in another 6-well dish to observe colony formation (Figure 10). Medium was replaced 2 times per week for 1 month until colonies had formed. Medium was then removed, and cells were rinsed twice with PBS and stained with Coomassie Blue dye. Colonies were viewed under phase contrast microscopy and Image J software was used to score the number of colonies, which were defined as a group of cells >25 cells.



4.6 Standardization of the MTT *in vitro* cytotoxicity assay:

The MTT cytotoxicity assay is a standard colorimetric assay that measures cell proliferation and is commonly used to determine toxic potential of various agents (Z. Wang, Butt, Wang, & Liu, 2007). The tetrazole MTT (3-(4,5-Dimethylthiazol-2-yl)-2,5-diphenyltetrazolium bromide) is reduced to purple formazan crystals in the mitochondria by the enzyme mitochondrial dehydrogenase, and these crystals can be solubilized and analyzed for absorbance (Carmichael et al., 1987). This assay is most sensitive when the cells are in log growth phase, and so optimal plating densities and incubation lengths must be determined prior to the cytotoxicity assays. Cells were seeded in 100ul media/well using a serial dilution of concentrations ranging from 250 to 35000 cells per well with eight replicate wells per dilution. The cells were allowed to adhere overnight,

and an additional 50 µl of media was added to each well as to replicate the MTT protocol. Cells were incubated for 24 hours or 4 days, at which point 15µl MTT (5 mg/ml) was added. The plate was incubated for an additional four hours, at which point the medium was removed, and formazan crystals were dissolved in 50 µl DMSO. The absorbance values were read on a microplate reader (Powerwave xs, Biotec) at two wavelengths, 570 nm and 650 nm. This standard curve was used to determine optimal seeding densities for MTT assays to obtain an absorbance between 0.7 and 1.25.

4.7 MTT in vitro cytotoxicity assay

MCF-7 cells were seeded in each well a 96-well plate at the optimal cell concentration per well, as determined from the standard curve for each cell line. Cells were treated with serial dilutions 0.001-10uM conventional (CrEL) taxol. Untreated cells were used as a control. All cells were cultured and absorbance values were quantified as previously discussed (section 4.6). Empty wells containing medium and MTT only were used as a blank and subtracted from absorbance values. Absorbance values for treated cells were reported as a percentage of the untreated cells.

Part 2: Characterization of Liposomes

4.8 Preparation of liposomal paclitaxel:

Paclitaxel, phospholipids and in some cases cholesterol were dissolved in a 50 ml round-bottomed flask and dried with a rotary evaporator (Buchi Rotavapor R 205) at a temperature above the T_c of phospholipids (i.e 33 °C for DMPC, 50 °C for DPPC and 65 °C for DSPC) under controlled vacuum (370 mbar) (Buchi Vacuum Controller V-800,

Brinkman, Toronto, ON, Canada) and flashed with a nitrogen stream to eliminate traces of chloroform. Briefly, phosphatidylcholine (DMPC; DPPC; DSPC) and phosphatidylglycerol were mixed at a 9:1 molar ratio and paclitaxel was added to a final ratio of 3.33 mol % with respect to total phospholipids. The lipid/paclitaxel film was hydrated with 2 ml of phosphate buffered saline and sonicated for 2 min (cycles of 15 min run and 15 min pause) (Sonics & Materials VC 50). To remove non-incorporated paclitaxel, the liposome solution was submitted to centrifugation at 18,000 x g for 10 min. In these conditions, small-sized liposomes remained suspended in the solution while free paclitaxel and large vesicles precipitated. The liposomal paclitaxel was then dialyzed overnight against PBS at 4°C with agitation to remove excess of unincorporated drug. The size distribution of liposomes was monitored by photon correlation spectroscopy using a Malvern 3000HS Zetasizer with He-Ne laser. The measurements were taken at room temperature at wavelength of 633.0 nm and 90° collecting optics.

4.9 Quantification of paclitaxel

The amount of paclitaxel incorporated in liposomes was determined by reversed phase HPLC. Drug content analysis was performed using a Symmetry C 18 column (Waters Nova-Pak C18 column) with a mobile phase containing a mixture of acetonitrile, water, and methanol (58:37:5, v/v/v) at a flow rate of 1 ml/min. Sample injection volumes were 20 µl and paclitaxel detection was performed using UV detector at a wavelength of 232 nm. Total run time was set to 5 min and paclitaxel retention time was 2.5 min. Peak area was recorded and processed.

Briefly, small amount of liposome solution (100 μ l) which contained entrapped paclitaxel was destroyed by acetonitrile solution (900 μ l). After sonication and centrifugation, the supernatant was subjected to HPLC for quantification of entrapped drug. The equation (2) can be used to calculate the entrapment efficiency.

$$(2) \text{ Drug entrapment efficiency} = (\text{Drug}_{\text{entr}} / \text{Drug}_{\text{total}}) \times 100$$

4.10 Drug release study

Paclitaxel leakage from liposomes was determined by a dialysis method. Briefly, 2 ml of liposomal paclitaxel was transferred into dialysis bags and dialyzed against 500 ml PBS with agitation at 37 °C. Each day the dialysis bags were transferred into new bottles containing 500 ml of PBS. Paclitaxel released from liposomes was successfully extracted with DMSO. The solvent was removed by nitrogen gas and the samples were reconstituted with 1ml acetonitrile and analyzed for drug content by HPLC method. Liposomal sizes were monitored throughout the release study using monitored by photon correlation spectroscopy using Malvern 3000HS Zetasizer with He-Ne laser and 90° collecting optics.

4.11 Rehydration of DPPC:DMPG liposomes:

Liposomes were composed of 38 mg DPPC:4 mg DMPG. DMPG, dimyristoyl phosphatidylglycerol was added to increase the stability of liposomes, consequently reducing the leakage of taxol from the liposomal formulation). Liposomes were maintained in a dehydrated lipid film for long-term storage at -20°C to retain stability. To rehydrate the lyophilized liposomes for use, 100 μ l of sterilized water was added and the

mixture was vortexed until all powder was dissolved. After 15 minutes at 45°C, 100 µl of PBS was added, and the sample was placed back at 45°C for additional 30 minutes. 300µL of PBS was added for a final volume of 500 µL. The mixture was vortexed throughout the procedure to ensure uniform composition and to eliminate any large clumps. The mean size of the liposomes after rehydration was 155nm, as determined by photon correlation spectroscopy using the Malvern 3000HS Zetasizer with He-Ne laser and 90° collecting optics.

4.12 Toxicity of Liposomes:

The MTT cytotoxicity assay was used to determine the toxicity of empty DPPC:DMPG liposomes on MCF-7 cells, as well as on the non-cancerous cell line, HSF-55. This study was carried out to ensure whether the lipid components of the liposomes contributed to the toxic effects of taxol.

Part 3: Evaluation of the effects of CrEL vs. liposomal taxol

4.13 DNA isolation

Cells were pelleted by centrifugation at 2000Xg and at 4°C. The medium was removed and the cells were resuspended in 100 µl nuclei buffer (Appendix A). After 10 minutes at 4°C, nuclei were pelleted by centrifugation at 10000 rpm for 5 minutes and 4°C. One hundred µl of phenol was added to the cytoplasmic fraction and was centrifuged at 14000 rpm for two minutes. The pellet was resuspended in 5 µl of 5 M NaCl, 15 µL sodium acetate, and 200 µl of 100% cold ethanol, and DNA was allowed to precipitate for at least 24 hours at -20°C.

4.14 DNA fragmentation assay:

DNA fragmentation is a known hallmark biochemical change induced by taxol (Au, Kumar, Li, & Wientjes, 1999). To determine the level of DNA fragmentation in MCF-7 cells, 5.0×10^5 cells were seeded in a 10 cm plate for each treatment or control sample. Cells were treated with serial concentrations of 0.1-10 μ M liposomal or conventional taxol. Cells incubated without any liposomes or drugs were used as controls. After 72 hours incubation, DNA was isolated from floating cells as described above (section 4.13). Following precipitation of DNA, samples were centrifuged at 11800 rpm for 15 minutes at 4°C. DNA pellets were resuspended in 20 μ l of water and separated on a 1.6% (w/v) agarose gel. DNA degradation was viewed and assessed visually with a UV transilluminator.

4.15 Flow cytometric cell cycle analysis of taxol-treated cells:

Flow cytometry is widely used to analyse the cell cycle of mammalian cells (Nunez, 2001; Potter et al., 2002). Cells were plated at a density of 75% confluence in a 100 mm dish and serial dilutions of taxol were added to the plates. The cells were incubated for 1-7 days, at which point the adherent cells were trypsinized and pooled together with floating cells. The floating cells were included in the analysis in order to accurately quantify cell death, as these cells have been shown to be crucial in the analysis of apoptosis (Turco, De Angelis, Stamatii, & Zucco, 2000). After being centrifuged at 200Xg for 6 minutes, the supernatant was removed and the cell pellet was resuspended in 0.5 ml PBS. Next, MCF-7 cells were put through a 25 gauge syringe to ensure a uniform, single-cell suspension. This step was not necessary for A549 cells, as they naturally form

a single-cell suspension upon trypsinization. Next, 4.5 ml of 70% (v/v) ethanol fixative was added to each tube containing PBS while the mixture was vortexed. Cells were stored at 4°C until staining and analysis for flow cytometry, at which point ethanol-suspended cells were centrifuged for 5 minutes at 200Xg. The ethanol was decanted and the cell pellet was resuspended in 5 ml PBS with 0.1% SDS. Next, 9 µl of propidium iodide (PI) staining solution [1 mg/ml PI, 10mg DNase-free RNase, 10 ml 0.1% (v/v) Triton X-100 in PBS] was added, and samples were incubated for 15 minutes at 37°C before analysis by flow cytometry (FACS; BD Biosciences).

Flow cytometry data were collected and analyzed using CellQuest Pro software (BD Biosciences). Control samples were used to determine and set gates for cell cycle analysis (sub-G1, G₀/G1, S, G2). The same software was used to determine the number of cells in each phase of the cell cycle, as well as the percentage of the total cells acquired in each region, based on the gates. P-values were obtained by performing unpaired Student's t-tests between data for G₂/M and sub-G1 following CrEL and liposomal treatments.

4.16 Determination of mitotic index:

The mitotic index was determined to verify flow cytometry data and to differentiate between cells in G₂ and those in mitotic arrest induced by taxol. This is a common technique used to quantitate the effects of taxol and other mitotic-inhibitor agents (Calastretti et al., 2001; Kamath et al., 2005; Schmidt et al., 2000). Cells were plated on glass coverslips in each well of a 6-well dish and allowed to adhere overnight. The following day, they were treated with 1 or 10 µM taxol for 24 hours. Treatment

length was determined by flow cytometry in order to determine a time-point where cells were still adherent and predominantly in G₂ arrest (Potter et al., 2002). Untreated cells were used as controls. Following treatment, the cells were fixed with ice-cold methanol. The cells were stained with 1 µg/ml 4',6-diamidino-2 phenylindole (DAPI) and mounted onto a microscope slide in mounting medium (90% (v/v) glycerol, 10% (v/v) 1 X PBS, containing 1 mg/ml p-phenylenediamine). Epifluorescence microscopy (Zeiss, North York, ON, Canada) was used to count a minimum of 500 cells per treatment and mitotic figures were scored. Mitotic figures were classified based on the appearance of chromatin condensation, and separation of discrete DNA molecules (Wang et al., 2005). P-values were obtained by performing unpaired Student's t-tests between data for CrEL and liposomal treatments.

4.17 Ultra-Performance Liquid Chromatographic analysis (UPLC) of relative taxol uptake:

Cells were plated at a density of 5×10^5 cells per 10 cm plate and treated with 10 µM liposomal or conventional paclitaxel. Plates were left to incubate for 24 hours, after which media was removed, cells were rinsed twice with PBS, trypsinized, and resuspended in media. Twenty µl of each sample was diluted in trypan blue dye. These were counted using a haemocytometer and brightfield microscopy to determine a total cell count for each sample. Next, the cells were pelleted at 3000 rpm for 10 minutes (Eppendorf). The supernatant was removed, and the cell pellet was frozen at -20°C until analysis. Cell pellets were thawed and resuspended in 100 µl mobile phase (58% (v/v)

acetonitrile, 37% (v/v) H₂O, and 5% (v/v) methanol) for analysis by ultra-performance liquid chromatography (UPLC; Waters).

Next, cells were sonicated at 75% intensity for 3 minutes to release taxol from the cells. Cell debris was pelleted at 14000 rpm for 2 minutes. Taxol was extracted according to a modified protocol developed by Yonemoto et al. 2007. Briefly, the supernatant, containing taxol, was transferred to a new tube and 1ml tert-butylmethyl ether (t-BME) was added. Samples were vortexed for one minute, then centrifuged for an additional 5 minutes at 1700 rpm. The organic supernatant was removed and transferred to a new tube. The t-BME was evaporated and residue was re-dissolved in 100 µl mobile phase. Samples were separated through a reverse-phase column (C18, 1.7 µm, bead diameter 1.0 x 50 mm; Waters) and analyzed at a wavelength of 229 nm at a flow rate of 0.25 ml/min. Data was analyzed using Waters Acquity software.

4.18 MTT analysis of the role of caspases in taxol-induced apoptosis:

To further elucidate the mechanism of cell death induced by taxol in MCF-7 breast cancer cells, the MTT cytotoxicity assay was used to test the efficacy of caspase-inhibitors as apoptosis-inhibitors (Yano et al., 2007). Caspases are important components of apoptosis and execution pathways, and have been shown to play a role in chemotherapy-induced cell death (Janicke et al., 1998; Ofir et al., 2002; S. J. Park et al., 2004). Cells were seeded in a 96-well plate and treated with taxol in combination with the caspase-inhibitors C1 (Caspase inhibitor 1: pan-caspase inhibitor of all caspase-1-like proteases; Calbiochem) or C3 (Caspase 3 inhibitor 1: inhibits caspases 3,6,7,8,10 & PARP cleavage; Calbiochem). Cells treated with the caspase-inhibitors or taxol were

used as controls. All absorbance values were reported as a percentage of the untreated control sample.

4.19 Western Blot analysis of P-glycoprotein (P-gp) in MCF-7 cells:

MCF-7 cells were seeded in a 100 mm plate at a density of 5×10^5 or 7×10^5 cells per plate for untreated and treated samples, respectively. After adherence, cells were treated with 10 μ M taxol or fresh medium for an additional 48 hours. Cells were trypsinized and pelleted and 400 μ l 2x sodium dodecyl sulphate (SDS) buffer was added to lyse the cells. Samples were boiled for 15 minutes and stored at -20°C until analysis. Next, samples were boiled for 15 minutes, and 25 μ l of each sample was loaded and separated by 10% (w/v) SDS-PAGE at 160 V. Protein was transferred to PVDF membrane at 30 V overnight at 4°C . The membrane was probed with C219 mouse monoclonal 1^o antibody (Signet) at 4°C overnight. The membrane was rinsed four times with TBST then probed again with anti-mouse 2^o antibody (Sigma). After another four rinses, the blot was rinsed in exposing solution and a film was exposed in the dark for 5 minutes and developed using an x-ray developer.

4.20 Statistical Analysis

The results were expressed as means \pm SEM obtained from three separate experiments. Comparisons were made by paired Student's t-test, and a *P* value of 0.05 or less was considered significant.

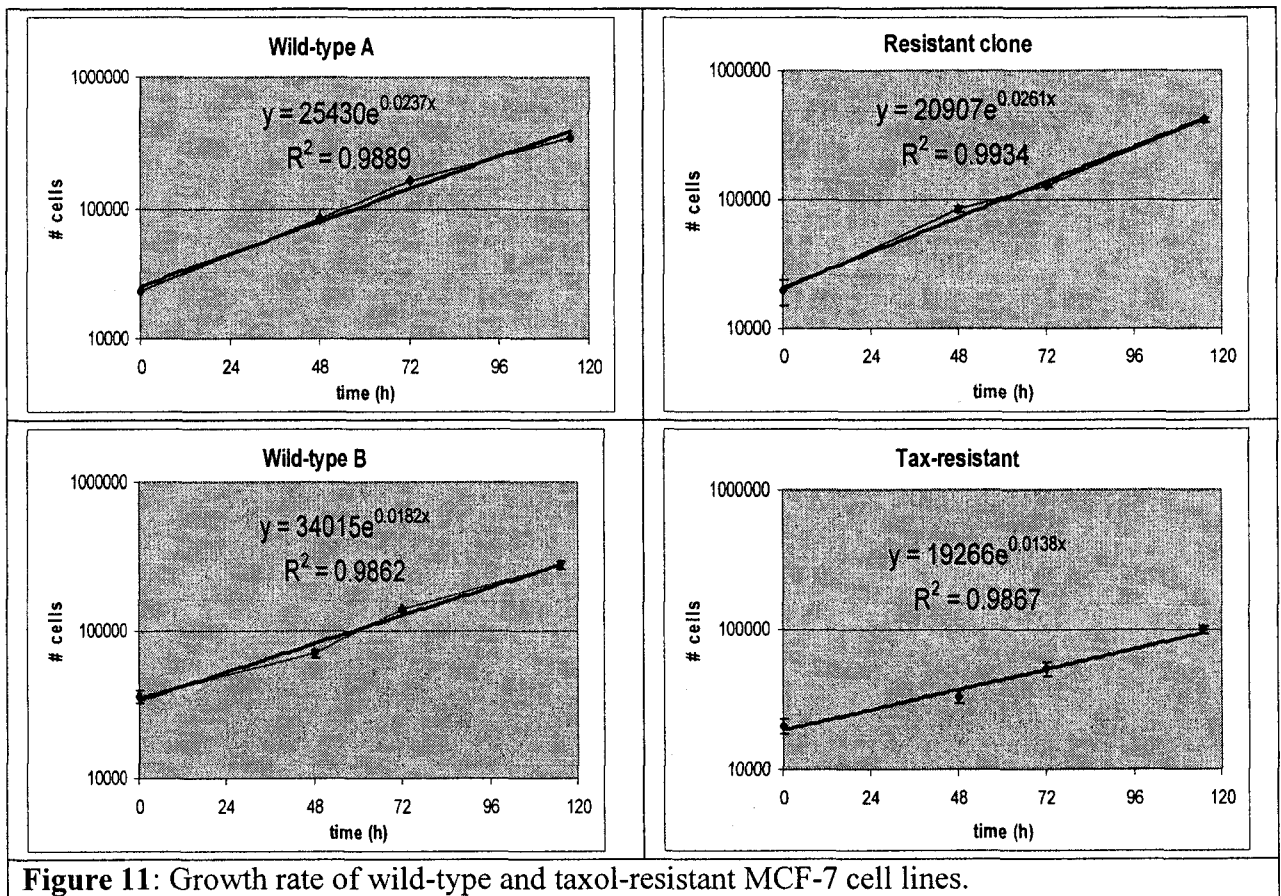
V. Results:

Part 1. Establishment of a taxol-resistant MCF-7 clone

Successive taxol treatments were used to establish taxol-resistant colonies of MCF-7 cells. In order to determine the length of a cell cycle and to characterize taxol-resistant cell lines in comparison to their parental counterparts, growth rates were calculated through a cell counting experiment (Figure 11). The doubling time for wild-type MCF-7 cells was 29.25 hours, which is the same as the ATCC value of 29 hours (Table 2; ATCC product information sheet, MCF-7 cells). A resistant sub-clone of the MCF-7 cells developed in our laboratory for this study had a similar doubling time to its wild-type counterpart (26.56 hours; Table 2). However, MCF-7 cells obtained from Dr. Parissenti had a significantly slower growth rate than this lot of cells (wild-type B, 38.09 hours). In addition, resistant cells derived from this cell line (tax-resistant) had a much slower growth rate than their wild-type counterparts (Tax-resistant, 50.23 hours; Guo et al, 2004). It is recognized that resistant cell lines typically have longer doubling times than their parental derivatives (35).

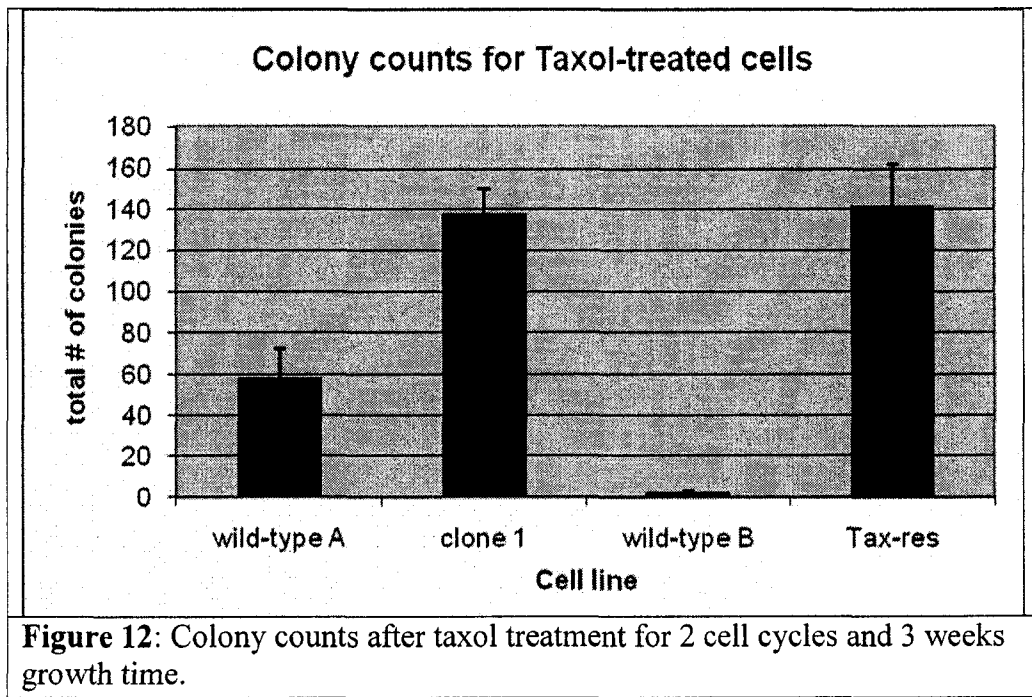
Doubling times were used as the length of a cell cycle for a colonization assay. In turn, this information was used to compare and characterize potentially taxol-resistant MCF-7 clones to their wild-type derivative (wild-type A), as well as to another MCF-7 strain (wild-type B) and another taxol-resistant MCF-7 cell line (tax-resistant). Cells were treated for two cell cycles, as determined from the doubling time, at which point they were allowed to recover in fresh medium. The number of colonies formed was counted and used to differentiate between potentially taxol-resistant colonies isolated

following successive taxol treatments, and those that were not resistant. Results for the most resistant clone are shown and compared to the two wild-type MCF-7 cell lines as well as the tax-resistant cell line (Figure 12). The MCF-7 clones isolated and selected from these experiments for their resistant properties were then used to test the efficacy of liposomal and conventional formulations of taxol, and to determine if liposomal encapsulation of taxol could enhance its ability to overcome resistance mechanisms in these cells.



Cell Line	Doubling time (hours)
Wild-type A	29.25 +/- 0.32
Clone	26.56 +/- 0.18
Wild-type B	38.09 +/- 0.53
Tax-resistant	50.23 +/- 0.67

Table 2: Comparison of doubling-time between wild-type MCF-7 cell lines and their taxol-resistant derivatives, as determined from growth curves.



Three strains of MCF-7 breast cancer cells were treated with a serial dilution of taxol for 4-days to determine and compare their sensitivity to the drug and to determine suitable concentrations of the drug for analysis with other assays. Standard curves were used to determine optimal plating density for 3 strains of MCF-7 breast cancer cells (wild-type A, clone, and tax-resistant) for the MTT cytotoxicity assay (Figure 13). Plating densities were determined by selecting a cell count coinciding with linear sensitivity of the MTT assay, with a preferable absorbance higher than 0.7 and lower than 1.25 (Table 3).

Wild-type MCF-7 cells had the lowest IC_{50} (0.008 μ M; Table 4), followed by a taxol-resistant clone (0.044 μ M; Table 4). The tax-resistant cell line had the highest IC_{50} of the three strains of MCF-7 cells (Table 4). Interestingly, the taxol-resistant clone was not highly resistant at lower concentrations, but did not show a linear response to taxol at higher concentrations. These results suggest a role for induced activation and expression of resistance genes, such as MDR1, by taxol at higher concentrations in this cell line and that concentrations of taxol of at least 0.1 μ M are needed to cause significant cytotoxicity in MCF-7 cells (Figure 14). As a result, concentrations ranging from 0.1-10 μ M were used in subsequent analyses.

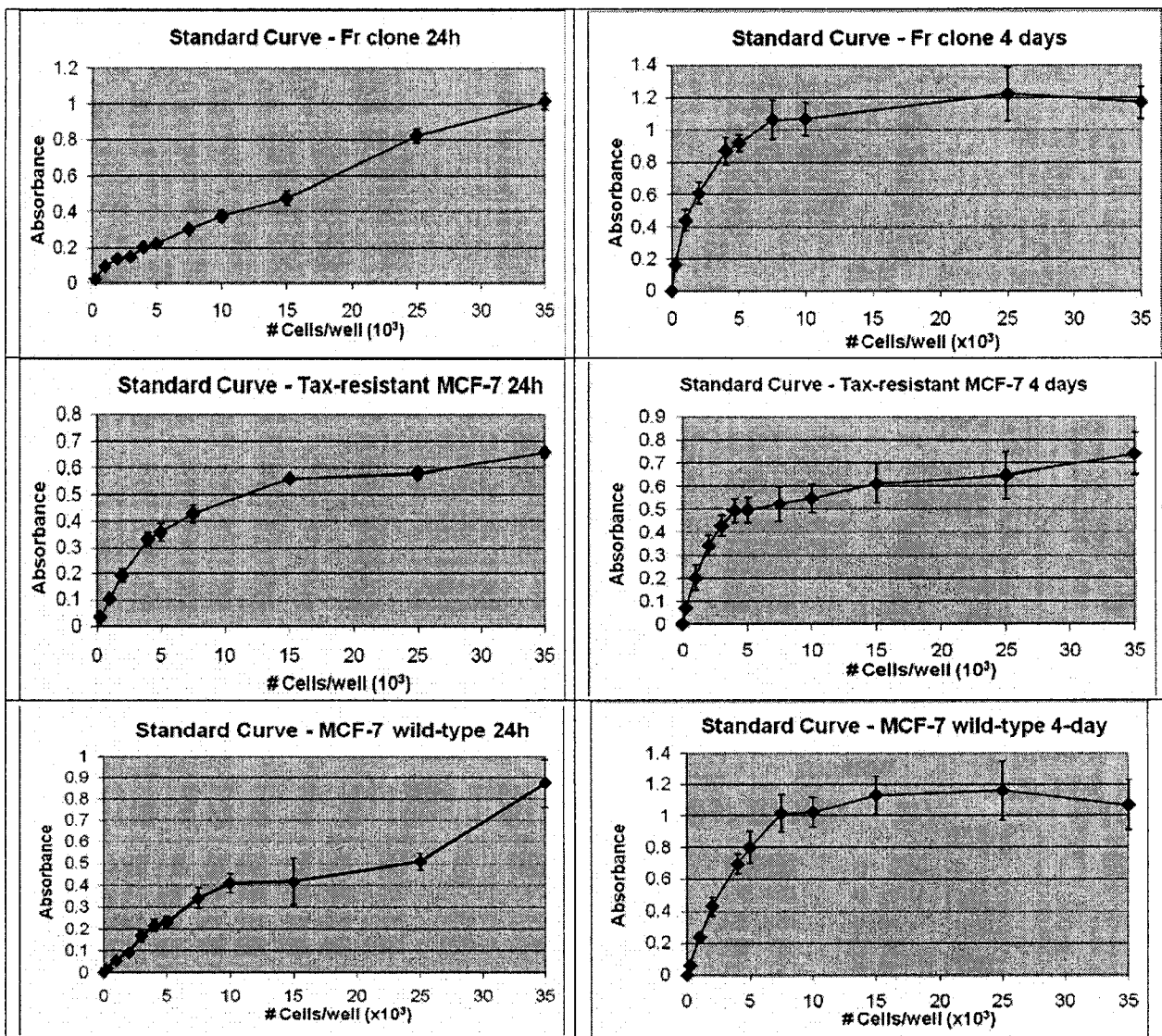


Figure 13: Standard curves for MCF-7 cancer cells to optimize initial cell densities for two end points using the MTT cytotoxicity assay.

Cell line	End-point (days)	Optimal seeding density (x10 ³)
MCF-7 clone	1	25
MCF-7 clone	4	2.5
Tax-resistant	1	3
Tax-resistant	4	2.5
Wild-type	1	10
Wild-type	4	4

Table 3: Optimal plating densities for cell lines used in this study for 1-day and 4-day end-points using the MTT cytotoxicity assay.

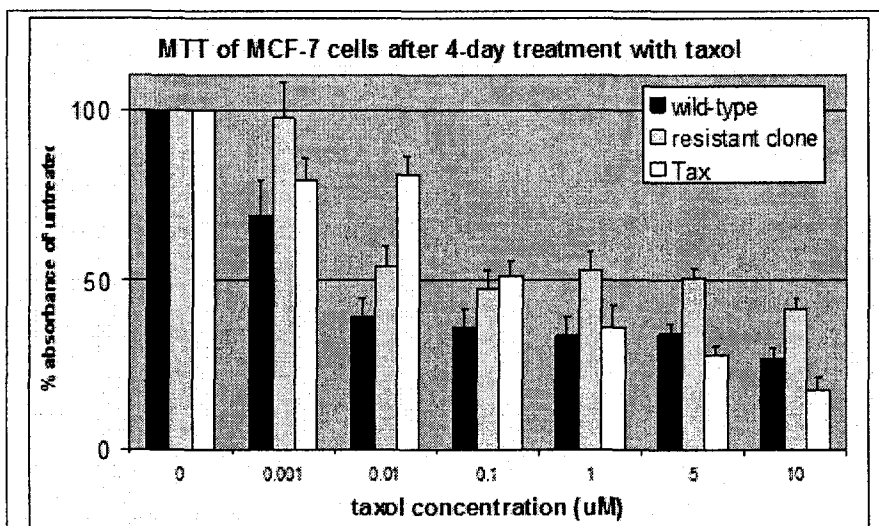


Figure 14: MTT analysis of 3 strains of MCF-7 breast cancer cells after 4-day treatment with taxol.

Table 4: IC₅₀ values for MCF-7 strains treated with taxol for 4 days as determined from MTT analysis.

Cell line (MCF-7)	IC ₅₀ (µM)
Wild-type	0.008
Resistant clone	0.044
Taxol-resistant	0.186

Part 2: Characterization of Liposomes

HPLC analysis was used to determine the cumulative release of taxol from three different formulations of liposomes over a period of four days (Table 5; Figure 15), as well as the stability of the liposomes (Figure 16). The stability of the liposomal taxol formulation is a percentage determined from the cumulative release, and it is important as it directly affects the half-life of the drug on the shelf, as well as the delivery of the drug to its target. These assays were used to determine the optimal formulation of liposomal taxol for storage and delivery of the drug. All three formulations, namely, DSPC-DMPG liposomes, DPPC-DMPG liposomes, and DMPC-DMPG liposomes retained comparable amounts of taxol (>97%, >95%, and >93% of taxol, respectively) (Figure 15).

Liposomes were analyzed by photon correlation spectroscopy throughout these studies. Taxol retention in liposomes can partially be attributed to liposome size, as the larger the liposome, the better the stability and taxol retention. The DPPC-DMPG liposomes were selected as the most favourable delivery method based on stability studies. The size distribution of this liposomal formulation is shown (Figure 17). A comparison of stability and mean size of the liposomal taxol formulations is summarized in Table 5.

MCF-7 and HSF-55 cells were treated with increasing concentrations of empty DPPC:DMPG liposomes for a period of 1-3 days to determine inherent toxicity of the lipids to cancer cells (MCF-7), as well as to non-cancerous tissue (HSF-55). An MTT assay was performed and the values were averaged for both cell lines. The liposomes were not found to be toxic, with >80% survival at the highest concentration (20 $\mu\text{l/ml}$; Figure 18).

Table 5: Full names of liposome formulations used in this study

Liposome	Full name of fatty acid component
DMPC-DMPG	dimyristoyl phosphatidylcholine: dimyristoyl phosphatidylglycerol
DPPC-DMPG	dipalmytoyl phosphatidylcholine: dimyristoyl phosphatidylglycerol
DSPC-DMPG	distearoyl phosphatidylcholine: dimyristoyl phosphatidylglycerol

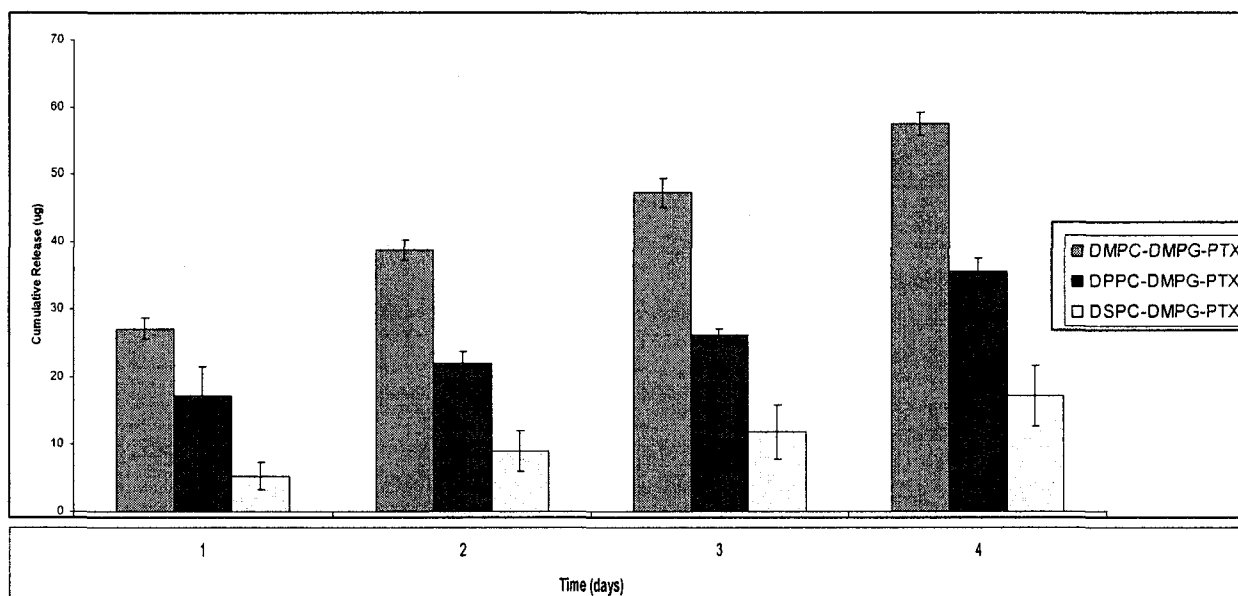


Figure 15: Cumulative release of paclitaxel (μg) from three formulations of liposomal taxol in phosphate buffer at 4°C .

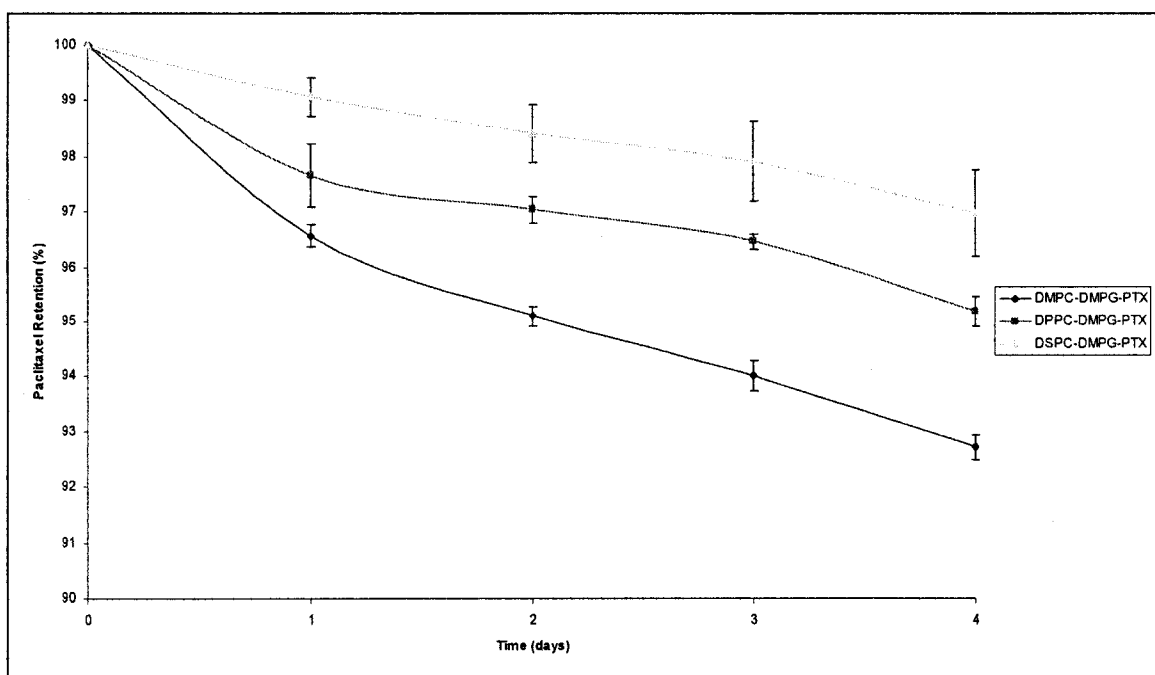


Figure 16: Stability of three formulations of liposomal taxol in phosphate buffer at 4°C as determined by HPLC analysis.

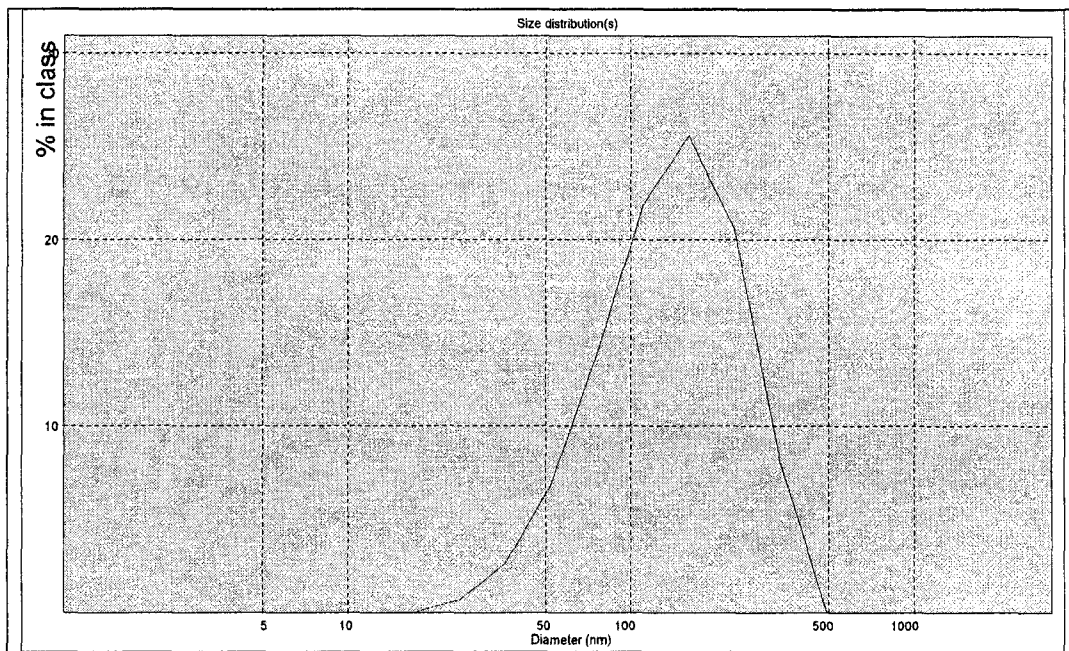
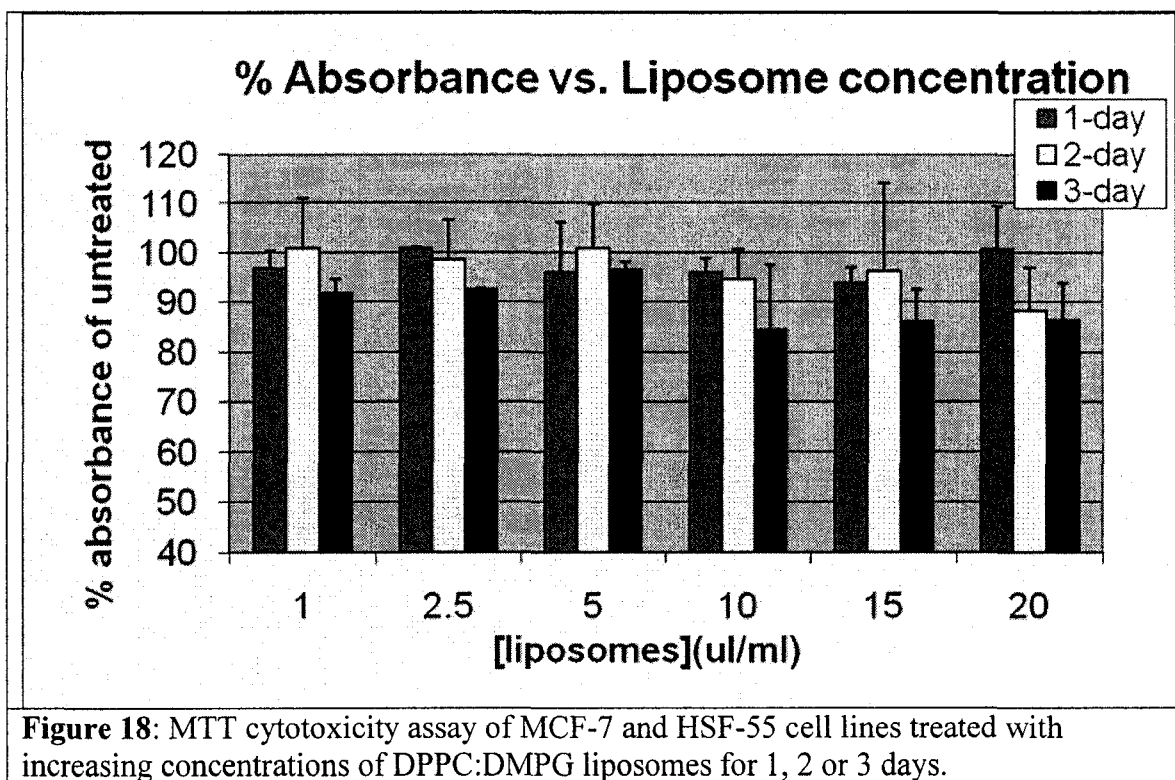


Figure 17: Size distribution of DPPC:DMPG liposomes as determined by photon correlation spectroscopy. Mean size = 155.7 nm.

Liposomes	Size (nm)	Poly. Ind.	Enc. Eff. (%)
DMPC-DMPG-PTX	143.07 ± 8.36	0.36 ± 0.01	96.10 ± 2.21
DPPC-DMPG-PTX	156.57 ± 3.58	0.39 ± 0.06	96.14 ± 5.77
DSPC-DMPG-PTX	184.93 ± 12.87	0.40 ± 0.05	70.18 ± 4.38

Table 5: Size distribution and encapsulation efficiency of liposomal taxol formulations as determined by photon correlation spectroscopy (PCS) and high performance liquid chromatography (HPLC).



Part 3: Evaluation of the effects of CrEL vs liposomal taxol

Taxol is known to cause mitotic arrest, leading to cell stress, and eventually cell death, or apoptosis (Moos and Fitzpatrick, 1998). In order to evaluate the effects of the two taxol forms, namely conventional (CrEL) and liposomal (liptax) on MCF-7 breast cancer cells, flow cytometric analysis of the cell cycle was used to determine the percentage of cells in G₂ or mitotic arrest, as well as the percentage of cells with degraded (sub-G₁) DNA. Mitotic indexes were also calculated to quantify and confirm the mitotic arrest induced by taxol, and DNA fragmentation analysis was used to determine the degree of apoptosis.

Flow cytometric analysis of MCF-7 cells treated with liposomal (liptax) or conventional (CrEL) taxol over a 7-day period was conducted to compare the effectiveness of the two formulations. Liposomal taxol treatment of wild-type MCF-7 cells demonstrated a slight increase in G₂ arrest when compared to the conventional formulation, up until 3-days incubation with the drug (Table 6a, Figure 19a). After this time-point, the liposomal formulation caused increased DNA degradation, which is indicative of cell death. This effect was seen most notably after 7 days incubation (68 versus 37% sub-G₁; Table 6a). Similar results were also seen following exposure of the clone cells and the tax-resistant MCF-7 cells to liposomal taxol (Tables 6b, 6c; Figures 19b, 19c).

Overall, this study revealed that liposomal taxol (liptax) caused G₂ arrest after shorter drug incubation lengths, and a greater percentage of cells underwent cell death (sub-G₁ cells) when compared to cells treated with conventional (CrEL) taxol. These effects were most prominent in a taxol-resistant clone.

% Total									
Region	control	day 1 CrEL	day 1 liptax	day 3 CrEL	day 3 liptax	day 5 CrEL	day 5 liptax	day 7 CrEL	day 7 liptax
sub-G1	8.15	3.78	8.98*	39.18	20.90*	16.42	44.04**	36.56	67.80**
G1/G0	59.30	24.88	14.78	15.72	10.19	19.49	7.87	15.28	5.57
S	9.11	8.29	6.75	4.83	9.81	11.95	7.00	9.12	5.35
G2/M	20.16	62.72	69.21	40.22	58.84*	52.45	40.70*	39.07	21.01*

Table 6a: Flow cytometric analysis of cell cycle – wild-type A MCF-7 cells treated with 10 μ M conventional taxol (CrEL) or Liposomal taxol (liptax). * indicates a significant difference between liposomal and CrEL treatments with $p < 0.05$ according to Student's t-test. ** indicates $p < 0.01$.

% Total									
Region	control	day 1 CrEL	day 1 liptax	day 3 CrEL	day 3 liptax	day 5 CrEL	day 5 liptax	day 7 CrEL	day 7 liptax
sub-G1	1.88	11.22	9.39	9.73	19.17*	13.51	46.28**	30.42	69.81**
G1/G0	78.28	42.64	30.95	42.05	22.66	41.54	15.15	33.98	10.30
S	7.06	6.07	8.79	5.75	6.21	4.29	5.00	4.19	3.62
G2/M	12.68	39.69	50.31	42.59	51.76*	40.52	33.02*	31.42	15.82*

Table 6b: Flow cytometric analysis of the cell cycle at different time points. Taxol-resistant MCF-7 clone cells were treated with 10 μ M conventional taxol (CrEL) or Liposomal taxol (liptax). * indicates a significant difference between liposomal and CrEL treatments with $p < 0.05$ according to Student's t-test. ** indicates $p < 0.01$.

		% Total							
Region	control	day 1 CrEL	day 1 liptax	day 3 CrEL	day 3 liptax	day 5 CrEL	day 5 liptax	day 7 CrEL	day 7 liptax
sub-G1		18.08	32.17**	9.73	19.17**	13.51	46.28**	30.42	69.81**
G1/G0	78.28	33.97	30.95	42.05	22.66	41.54	15.15	33.98	10.30
S	7.06	9.71	8.79	5.75	6.21	4.29	5.00	4.19	3.62
G2/M	12.68	37.72	50.31	42.59	51.76	40.52	33.02	31.42	15.82*

Table 6c: Flow cytometric analysis of cell cycle at different time points. Taxol-resistant cells were treated with 10 μ M conventional (CrEL) or Liposomal taxol (liptax). * indicates a significant difference between liposomal and CrEL treatments with $p < 0.05$ according to Student's t-test. ** indicates $p < 0.01$.

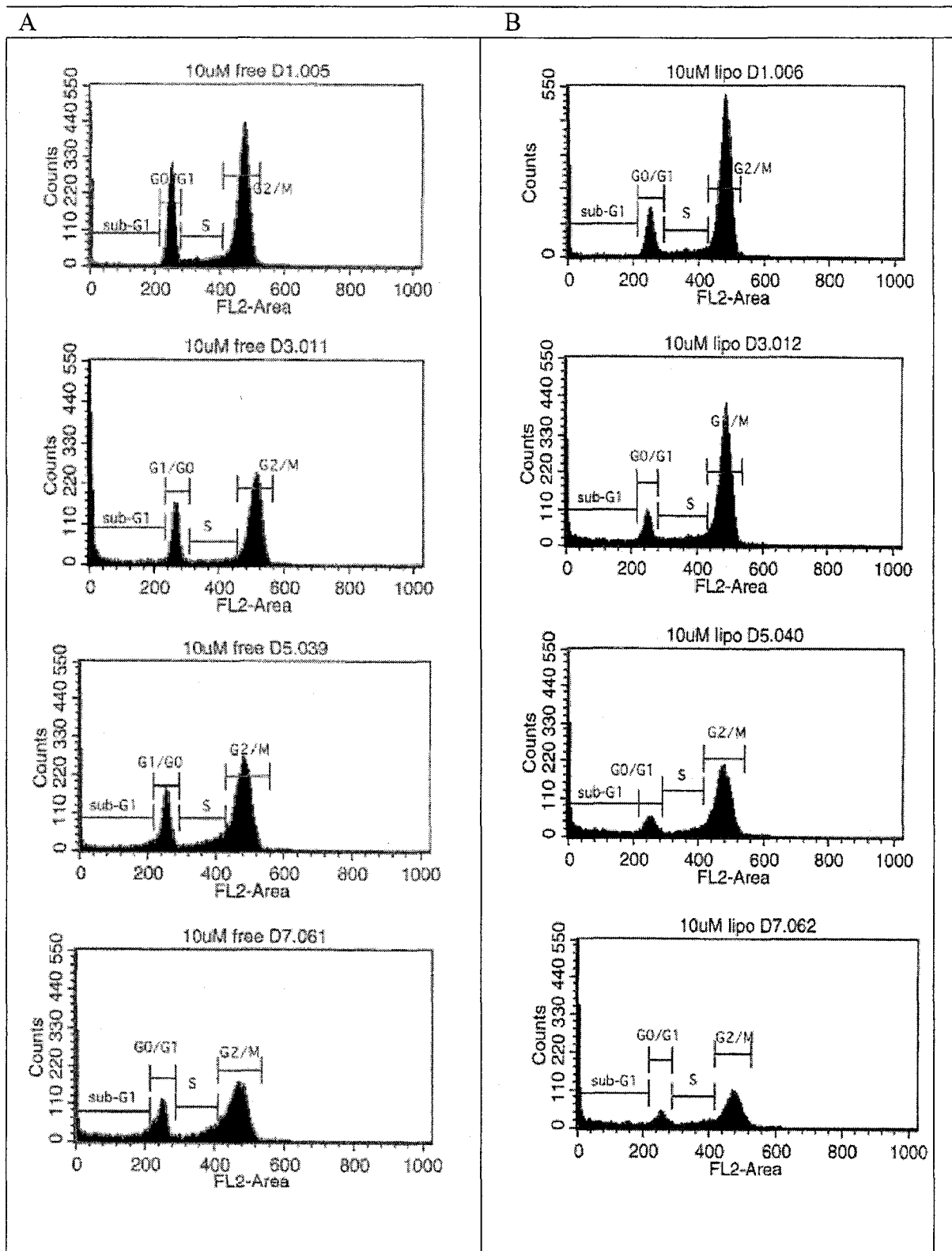


Figure 19a: Histograms showing the number of cells in each phase of the cell cycle for wild-type MCF-7 breast cancer cells after treatment with 10 μ M conventional (A) or liposomal (B) taxol over a 7-day period. Results are given for 1-day (D1), 3-day (D3), 5-day (D5) and 7-day (D7) incubation lengths in taxol.

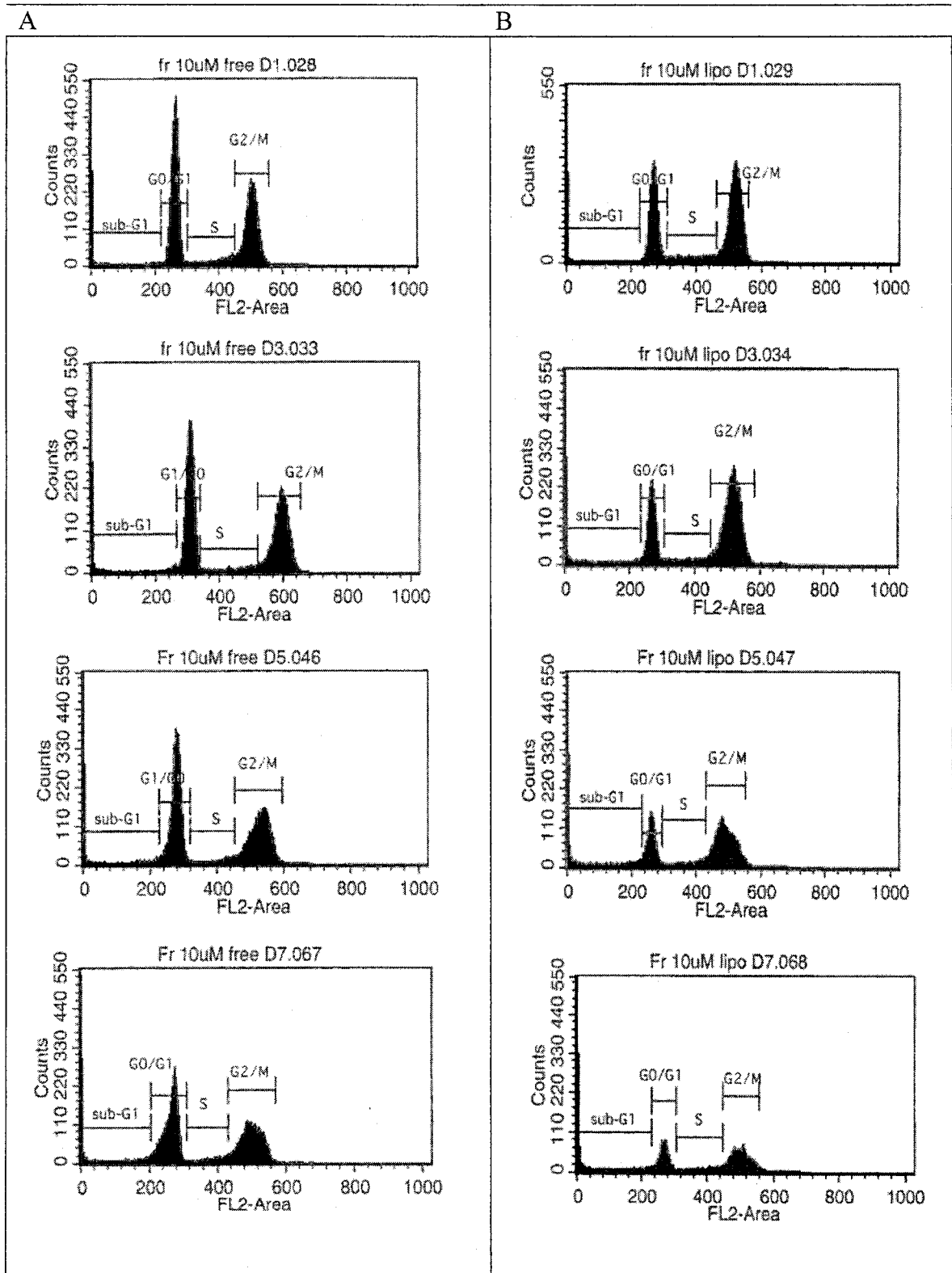


Figure 19b: Histograms showing the number of cells in each phase of the cell cycle for clone MCF-7 breast cancer cells after treatment with 10 μM conventional (A) or liposomal (B) taxol over a 7-day period. Results are given for 1-day (D1), 3-day (D3), 5-day (D5) and 7-day (D7) incubation lengths in taxol.

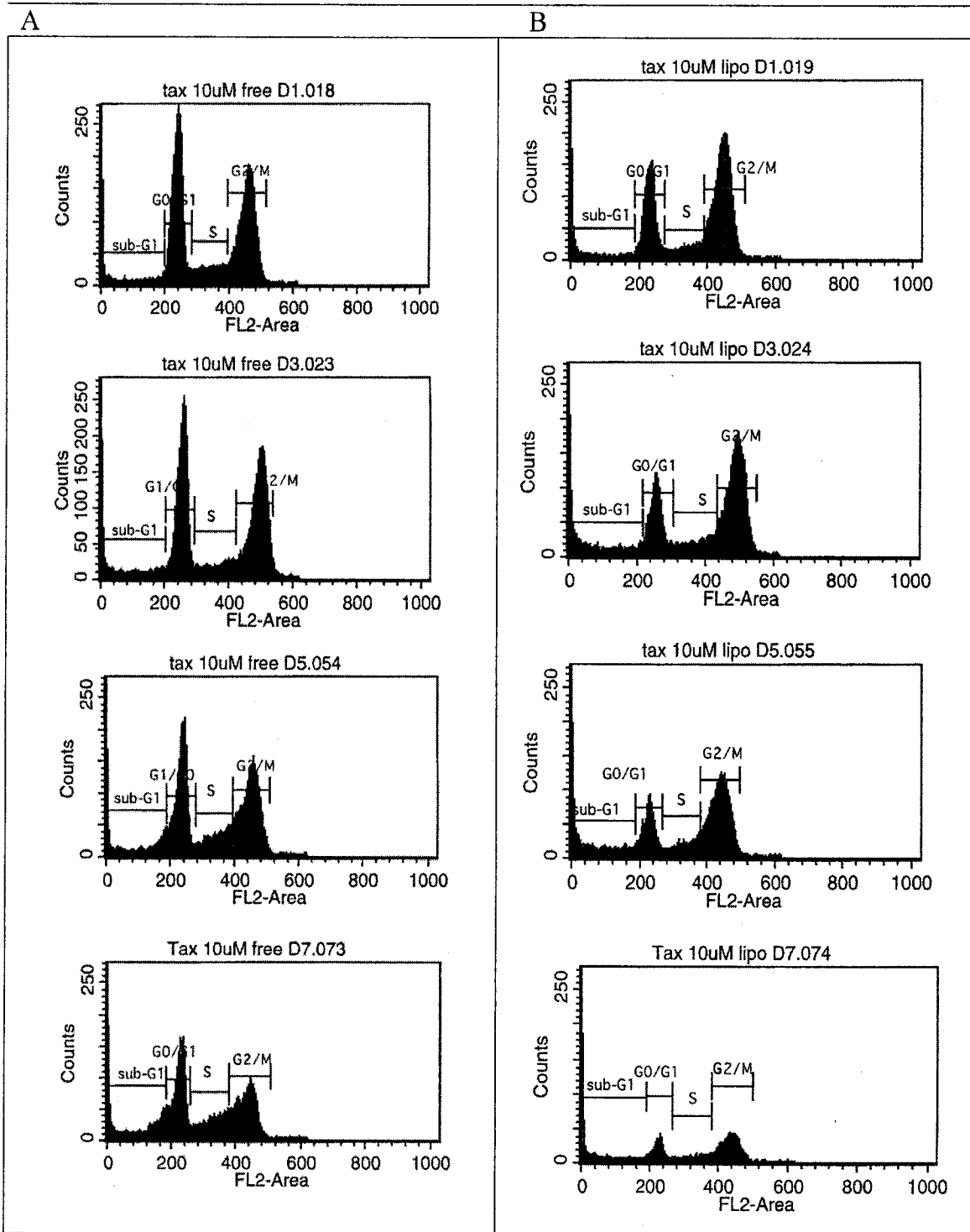


Figure 19c: Histograms showing the number of cells in each phase of the cell cycle for tax-resistant MCF-7 breast cancer cells after treatment with 10 μ M conventional (A) or liposomal (B) taxol over a 7-day period. Results are given for 1-day (D1), 3-day (D3), 5-day (D5) and 7-day (D7) incubation lengths in taxol.

Taxol is known to bind microtubules, inducing mitotic arrest in cells that eventually leads to cell stress and cell death (Moos & Fitzpatrick, 1998). As a measure of the effect of taxol on cancer cells, mitotic indexes were determined for wild-type and clone MCF-7 breast cancer cells treated with either CrEL taxol or liposomal taxol at 1 μ M or 10 μ M for 24 hours.

These results can differentiate between the G₂ and M (mitosis) phases of the cell cycle as determined by flow cytometry, to further correlate taxol treatment with mitotic arrest. Under normal, untreated conditions, dividing mitotic figures were observed in all stages of mitosis, including metaphase, anaphase, and telophase (Figure 20). In contrast, mitotic figures induced by taxol treatment were predominantly condensed chromosomes in metaphase.

MCF-7 breast cancer cells showed a significant increase in mitotic figures upon treatment with liposomal taxol when compared to CrEL taxol (Table 7). This increase was more dramatic at higher concentrations of taxol (10 μ M). Mitotic indices were not able to be reliably determined for tax-resistant MCF-7 cells, as these cells tended to form foci as they grow, and nuclei appeared layered on top of each other, even at low density. As a result, mitotic figures were not clearly visible, and total cell counts could not be ascertained.

Table 7: Mitotic index of control and taxol-treated cancer cells

Taxol (uM)	Mitotic Index (%)				
	0	1-CrEL	1-Liptax	10-CrEL	10-Liptax
MCF-7 wild-type	5	26.2	39.2	11.1	42.3**
MCF-7 clone	7.3	26.9	49.4	12.4	52.3**

Mitotic indices were determined following 24 hour taxol treatment.
** indicates significant difference between CrEL and Liptax treatment, where $p < 0.01$.

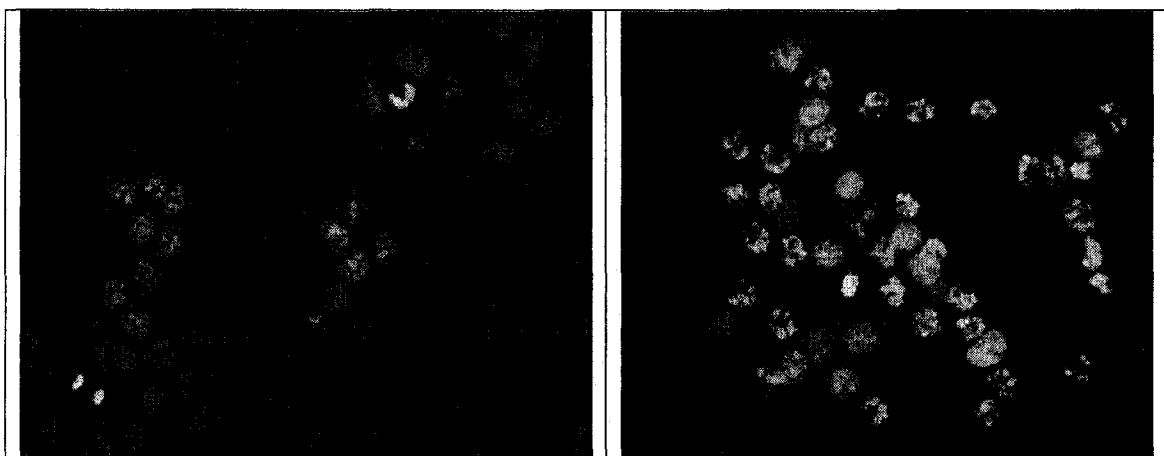


Figure 20: Wild-type MCF-7 breast cancer cells stained with DAPI and viewed under fluorescent light with a 40X objective under normal conditions (A), and after liposomal taxol treatment (B)

Following mitotic arrest, taxol is known to cause apoptosis (Moos & Fitzpatrick, 1998). DNA fragmentation is a known marker of apoptosis, and in certain cell types, cleavage of DNA into internucleosomal fragments of ~ 200bp can be visualized as a “DNA ladder” by gel electrophoresis (P. Huang, Robertson, Wright, & Plunkett, 1995).

MCF-7 breast cancer cells were treated with a range of concentrations of liposomal or conventional (CrEL) taxol, and DNA fragmentation was visualized by agarose gel electrophoresis (Figure 21a). This fragmentation was quantified and compared using computer analysis of gel bands. Results of DNA fragmentation assays showed that wild-type MCF-7 cells had the greatest amount of DNA fragmentation following treatment with taxol (26-36 mean CNT). However, there was no significant difference in the amount of fragmentation generated by either formulation.

There was a marked increase in DNA fragmentation in clone MCF-7 cells after treatment with 10 μ M liposomal taxol for 4 days when compared to equivalent treatment with CrEL taxol. Tax-resistant MCF-7 cells had very little fragmentation with either formulation, and as a result, there was no significant difference when comparing treatment with the two formulations (Figure 21a, Figure 21b).

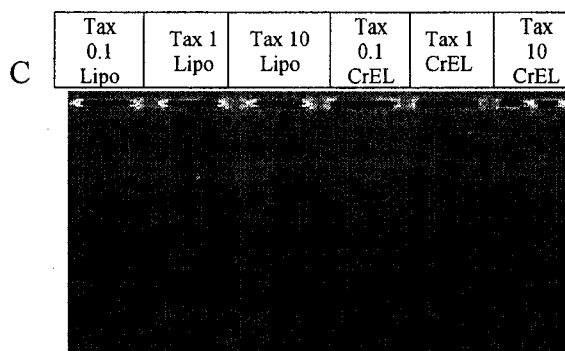
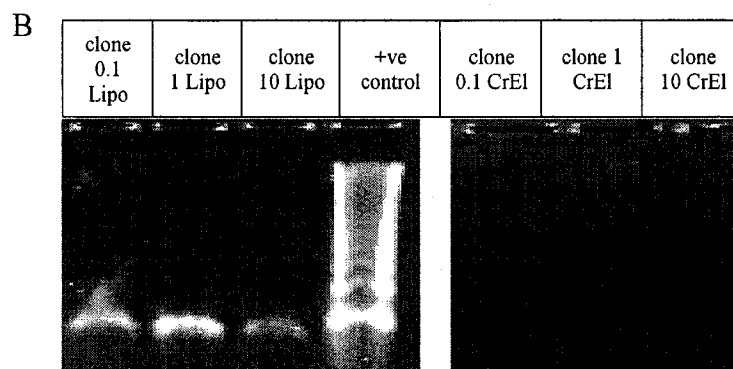
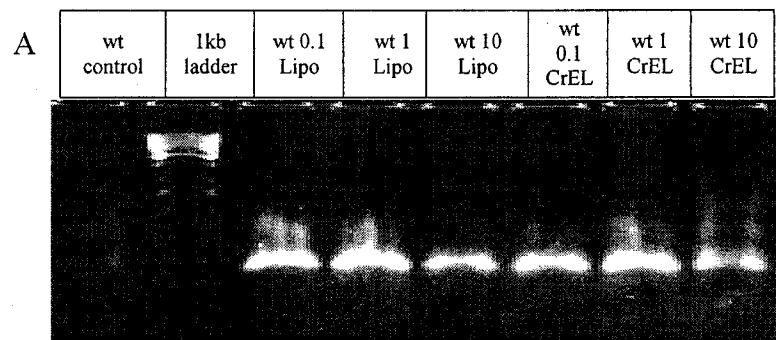
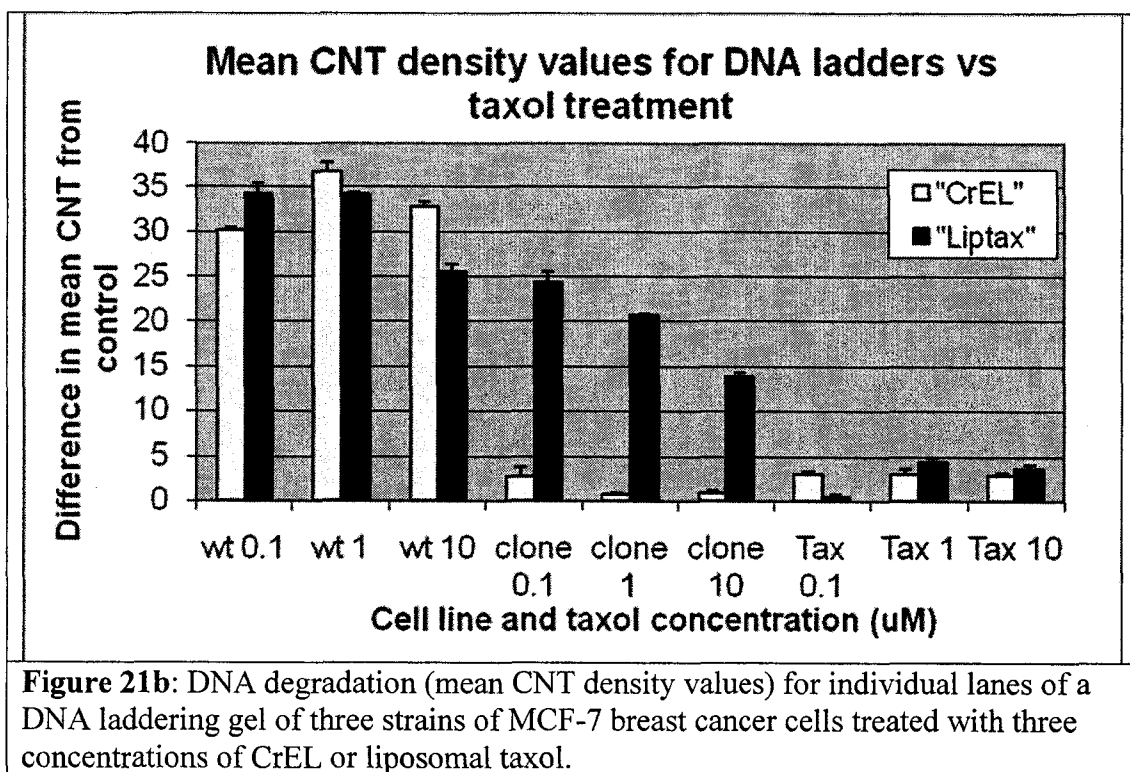


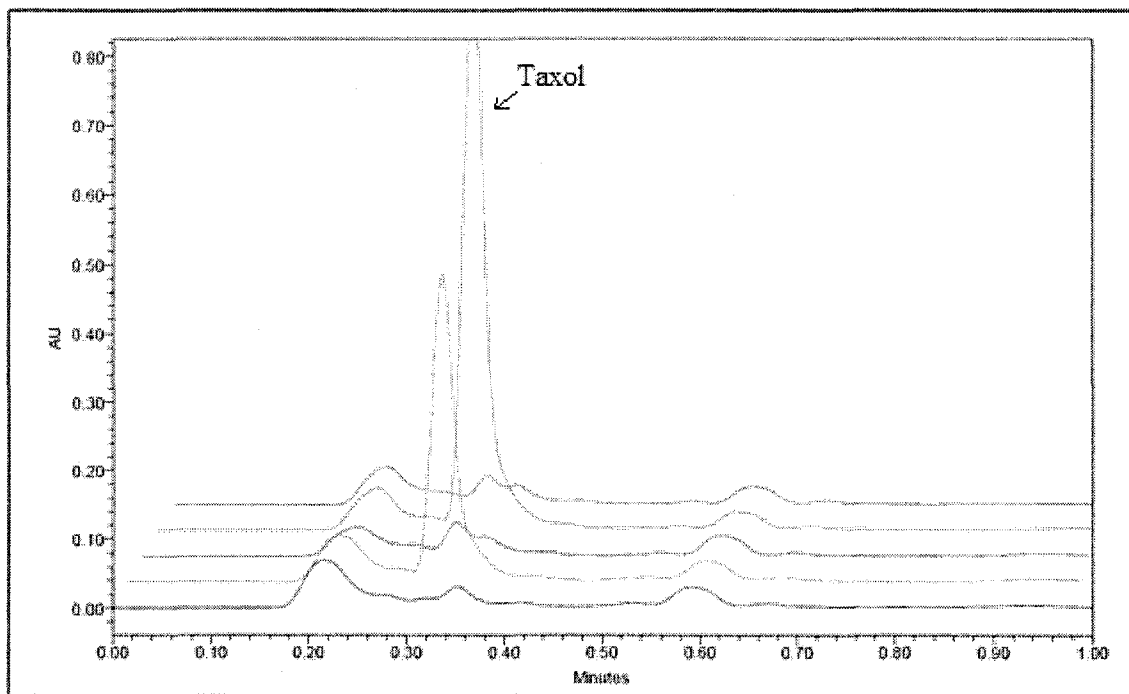
Figure 21a: DNA laddering gel demonstrating DNA fragmentation in wild-type (A), clone (B), or Tax-resistant (C) MCF-7 cells treated with 0.1, 1, or 10 μ M liposomal (Lipo) or conventional (CrEL) taxol.



In order to elucidate whether increases in taxol-induced changes in mitotic index, and apoptosis were related to the cellular concentration of taxol, the uptake of taxol, administered as a liposomal or conventional formulation by MCF cells, was measured by UPLC. The retention time of taxol was 0.320 minutes, with a maximum absorbance at 229 nm. A standard curve was automatically generated using Acquity software (Waters) for UPLC analysis of taxol using three separate concentrations of the drug (data not shown). Concentrations lower than 0.4 μM were not able to be accurately quantitated using this calibration, and as a result, they are reported as “not determined” (ND) in Table 8. This standard calibration was used to quantitate the amount of taxol in media and cell lysate samples treated for 24 hours with taxol.

The results from uptake studies revealed that the uptake of taxol by taxol-resistant cells was markedly higher in those cells challenged with liposomal (liptax). Media samples containing taxol were also analyzed after incubation with cells to determine residual taxol not taken up by cells after treatment. The results from those experiments showed that there was an association between changes in cellular levels of taxol and those measured in the media (Figure 22, Table 8). More precisely, the residual taxol in the media of samples incubated with liposomal taxol were lower than those observed following incubation with CrEL (data not shown).

Similar results were found for all three strains of MCF-7 cells, but interestingly, the most prominent difference was noted in the taxol-resistant cell lines (Figure 22). Samples that were not treated with taxol were used as a control to ensure that no components found in the media, buffer, mobile phase, or cell lysate interfered with the taxol peak eluting at 0.320 minutes.



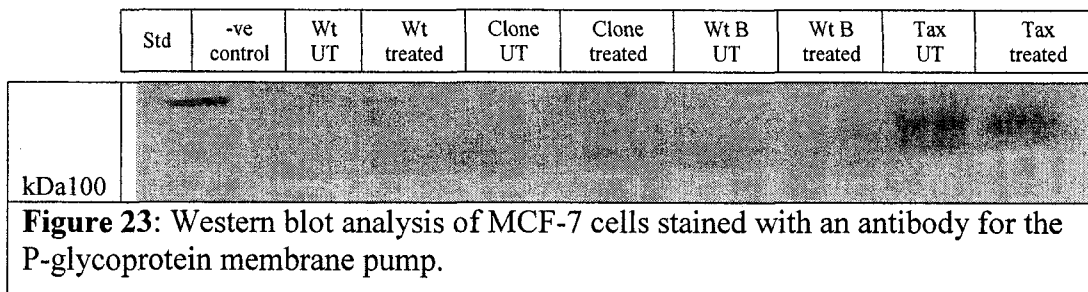
	Untreated control Tax cells Tax cells treated with Liptax Tax cells treated with CrEL taxol Clone cells treated with Liptax Clone cells treated with CrEL taxol
<p>Figure 22: UPLC chromatogram showing the level of taxol uptake of taxol-resistant cells treated with 10 μM taxol for 24 hours.</p>	

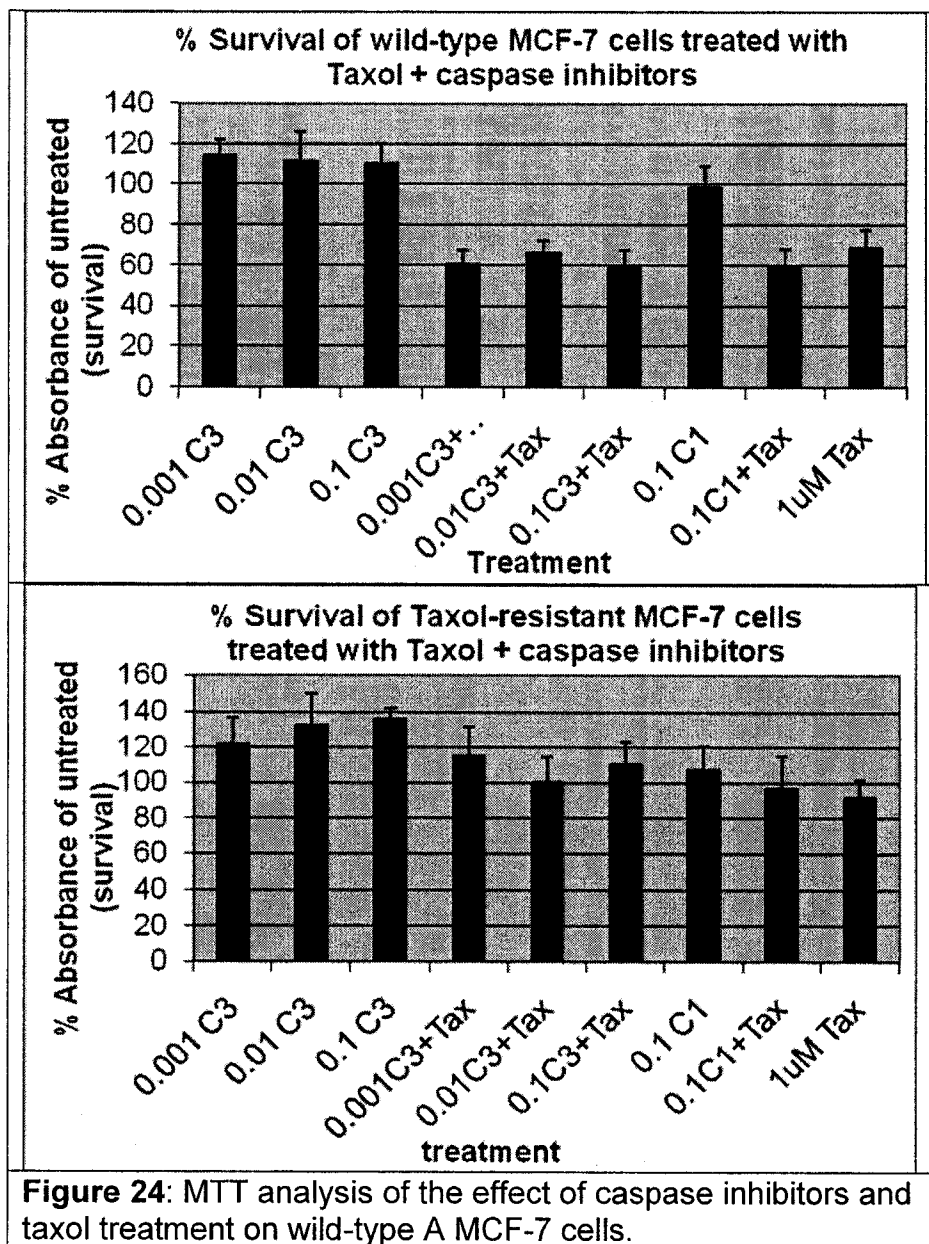
Sample	Taxol treatment	Retention time (RT)	Peak Area	Amount (μM)	Total # cells ($\times 10^6$)	Taxol (μM) per 1×10^6 cells
Tax control	Untreated	0.320	N/A	ND	1.5	ND
Tax	Liptax	0.321	730098	7.998	0.9	8.89
Tax	CrEL	0.320	60301	ND	0.9	ND
Clone	Liptax	0.322	1271345	19.305	2.7	7.15
Clone	CrEL	0.321	46472	ND	2.8	ND

Table 8: Taxol uptake as determined from UPLC chromatograms. Amounts could not be detected (ND) below $0.4 \mu\text{M}$.

To further elucidate the mechanism of cellular resistance to taxol in drug-resistant MCF-7 cells, the resistance protein encoded by MDR1, p-glycoprotein (P-gp) was assessed. Western blot analysis of MCF-7 cells detected the presence of the P-glycoprotein membrane pump commonly implicated in multidrug resistance. However, the protein was only detectable in a taxol-resistant cell line, and not in wild-type MCF-7 cells or a taxol-resistant MCF-7 clone (Figure 23). In addition, there was no difference in the level of expression in cells that were treated with taxol than the level of expression in untreated cells of the same cell line, suggesting that this pump is consistently expressed in these cells, and is not induced or upregulated by taxol treatment.

To further analyze the mechanism of cell death induced by taxol and to determine if the common apoptosis pathway involving the caspase signaling cascade is induced by the drug, an MTT cytotoxicity assay was performed on cells treated with taxol in combination with caspase inhibitors. The combination of caspase inhibitors and taxol had no effect on taxol-induced cell death, yet treatment with caspase inhibitors impacted spontaneous apoptosis, resulting in an increase in absorbance in these cells compared to untreated cells (Figure 24). This suggests that the predominant pathway of apoptosis in cycling MCF-7 cells involves the cleavage of caspases. However, taxol induces an alternate apoptotic pathway, and as a result, analysis of caspase activity is not an appropriate measure of taxol-induced cell death.





In order to determine the effect of liposomal taxol on other cell types commonly treated with taxol, A549 lung cancer cells were analyzed for their response to liposomal taxol in comparison to conventional CrEL taxol. Preliminary studies of cytotoxicity, cell death, and mitotic arrest were performed. Cytotoxicity was analyzed by MTT assays, which were standardized and performed after 24 hours and 5 days of incubation with the two formulations of taxol (Figure 25, Table 9, Figure 26). The results of this assay did not demonstrate any notable difference between the two formulations.

Flow cytometric analysis of the cell cycle was carried out to compare the level of G2 arrest and DNA degradation in the lung cancer cells following 24 hours of 1 μM or 10 μM taxol treatment (Figure 27, Table 10). After 1 μM taxol treatment, the two formulations had nearly identical effects on the lung cancer cells. However, after 10 μM taxol treatment, there was increased G2 arrest (80.90 versus 64.34%), and DNA degradation (sub-G1; 10.61 versus 5.33%) in the cells treated with liposomal taxol in comparison to those treated with conventional CrEL taxol (Table 10). These preliminary data suggest that the liposomal taxol might be more advantageous than the conventional treatment in the chemotherapy of lung adenocarcinoma.

The mitotic index was also determined for A549 lung cancer cells after 24 hour treatment with 1 μM or 10 μM taxol. Results from this assay demonstrated a similar outcome, as liposomal taxol caused increased mitotic index in these cells, and a greater difference was noticed at the higher concentration of taxol (Table 11).

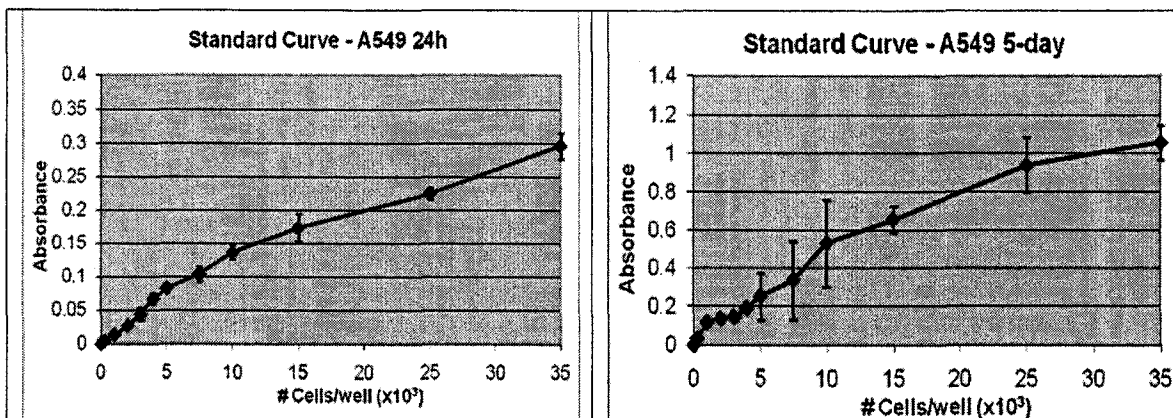
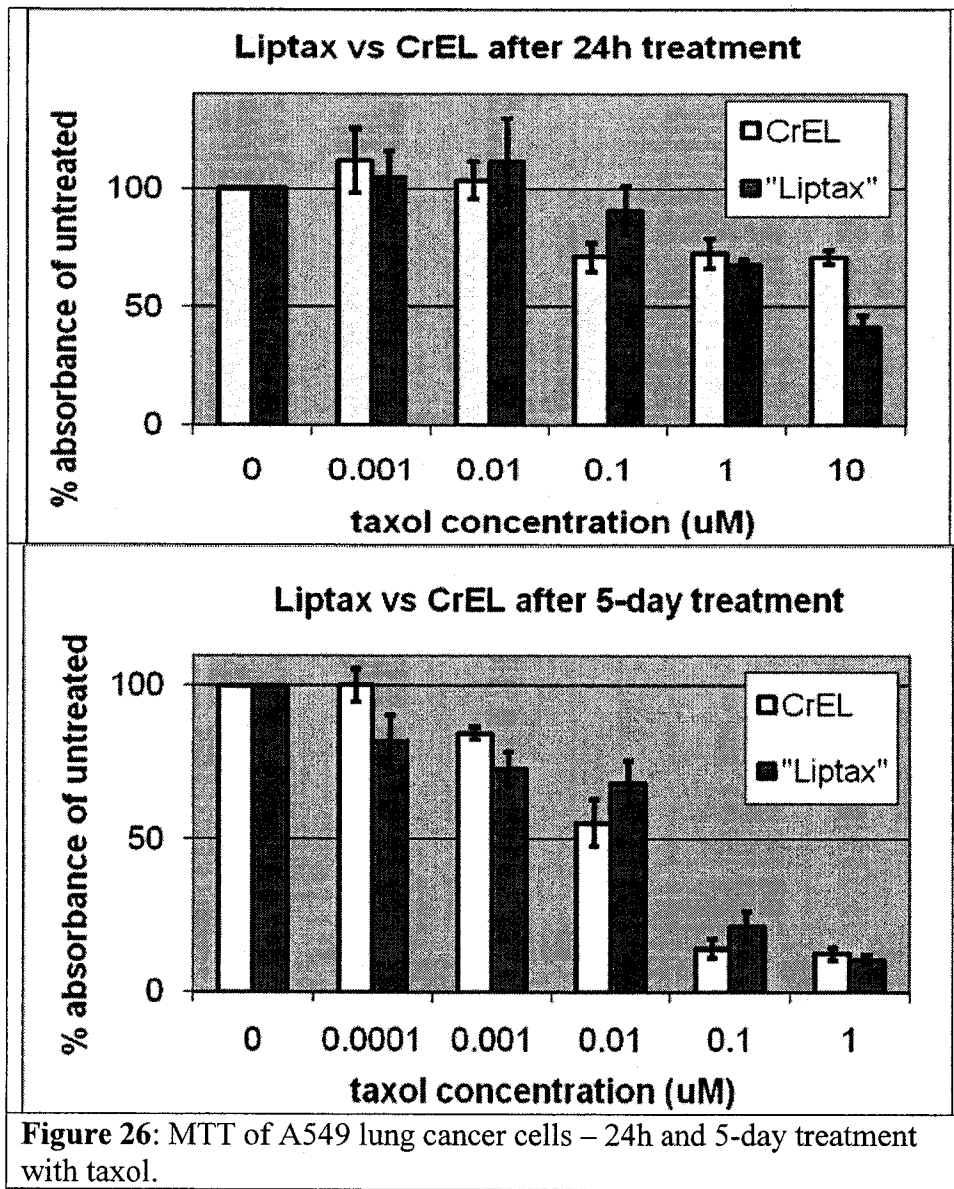


Figure 25: Standard curves for A549 lung cancer cells to optimize initial cell densities for two end points using the MTT cytotoxicity assay.

Cell line	End-point (days)	Optimal seeding density (x10 ³)
A549	1	25
A549	5	15

Table 9: Optimal plating densities for A549 lung cancer cells analyzed at 1-day and 5-day end-points using the MTT cytotoxicity assay.



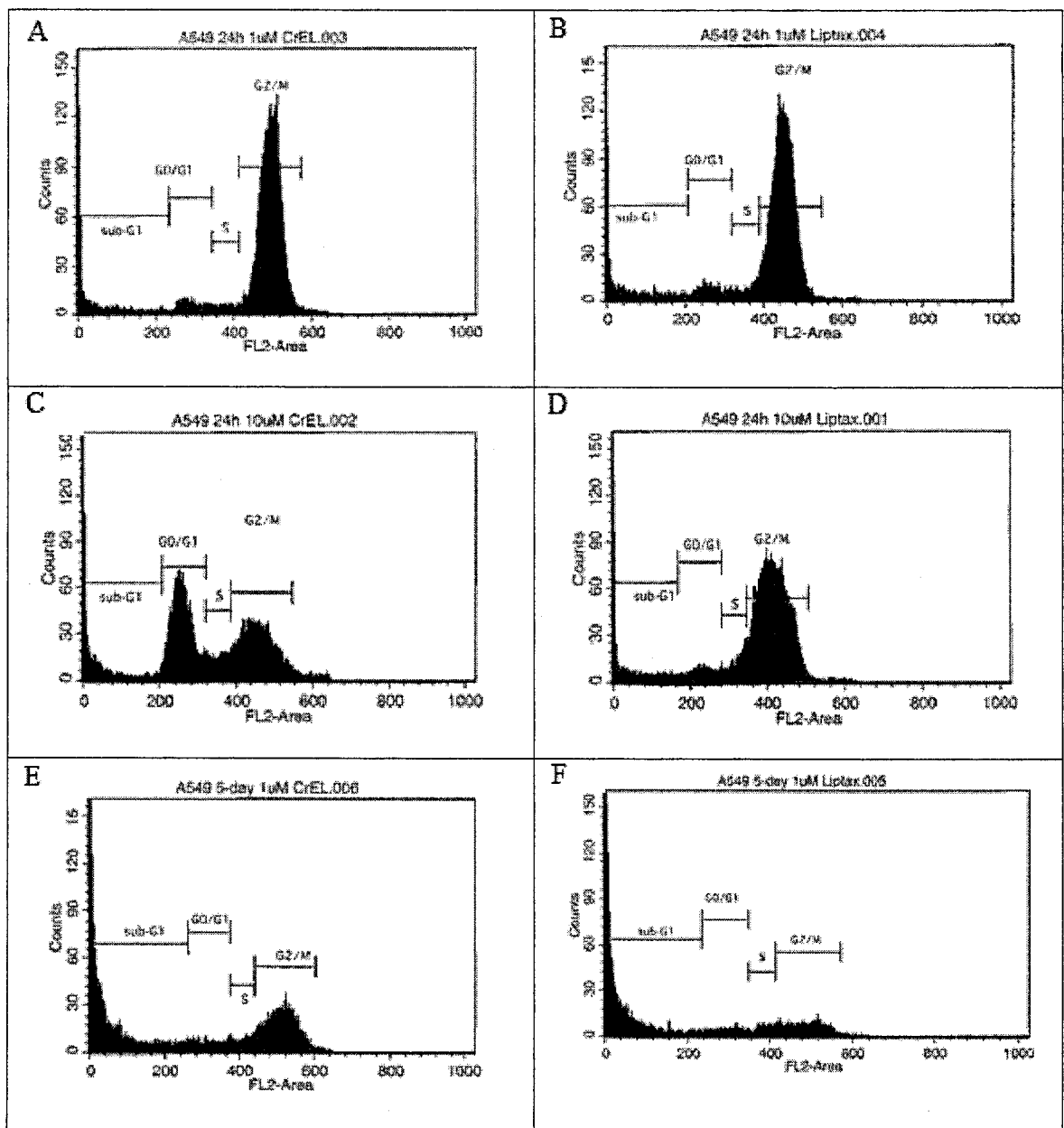


Figure 27: Flow cytometric analysis of A549 lung cancer cells treated with CrEL (A,C,E) or liposomal (B,D,F) taxol for 24 hours (A,B,C,D), or 5-days (E,F). All samples were treated with 1 μ M taxol, with the exception of C and D, which were treated with 10 μ M.

		% Total			
Region	control	24h 1	24h	24h	24h
		1 μ M CrEL	1 μ M liptax	10 μ M CrEL	10 μ M liptax
sub-G1	2.63	12.01	13.74	5.33	10.61
G1/G0	71.61	6.42	4.65	27.31	5.58
S	8.26	4.16	2.28	2.49	2.53
G2/M	17.65	77.13	78.45	64.34	80.9

Table 10: Preliminary flow cytometric cell cycle analysis of A549 lung cancer cells treated for 24h with 1 or 10 μ M conventional (CrEL) or liposomal (liptax) taxol.

Table 11: Mitotic index of control and taxol-treated cancer cells

Taxol (μM)	Mitotic Index (%)				
	0	1-CrEL	1-Liptax	10-CrEL	10-Liptax
A549 lung cells	3.9	68.2	74.2	46.1	56.5*

Mitotic indices were determined following 24 hour taxol treatment.

* indicates significant difference between CrEL and Liptax treatment, where $p < 0.05$.

VII. Discussion

A new formulation of liposomal taxol was developed in an attempt to explore alternatives to the current Cremophor EL (CrEL) vehicle, which is known to exert several adverse effects, including anaphylactic shock (Gelderblom et al., 2001; Gelderblom et al., 2001; Sparreboom et al., 1999; van Tellingen et al., 1999). Two taxol-resistant MCF-7 cell lines (tax-resistant and clone) were used to test the efficacy of liposomal taxol in comparison to the conventional CrEL formulation, as well as to determine whether liposomal encapsulation would circumvent the resistance mechanisms expressed by these cells. The two formulations were also tested on the parental wild-type MCF-7 cells, which are inherently sensitive to the drug.

A taxol-resistant MCF-7 clone was established through successive treatments with high concentrations of taxol over a period of several months. This clone had distinctive differences in growth characteristics, morphology, and sensitivity to taxol when compared to the parental strain of MCF-7 cells. Specifically, it had a shorter doubling time, cells appeared smaller in size and grew more densely in culture, and it displayed a non-linear response to taxol at concentrations $>0.01\mu\text{M}$. Another taxol-resistant MCF-7 cell line kindly provided to us by Dr. Parissenti also displayed altered growth characteristics, morphology, and taxol sensitivity (Guo et al., 2003; Guo et al., 2004; Villeneuve et al., 2006). However, there were differences between these two resistant lines. The tax-resistant line had a longer doubling time, and the cells appeared larger and less dense than the wild-type cells. These effects are not unusual, as altered morphology and growth characteristics have been encountered in other chemoresistant

cell models (Li et al., 2004). However, these taxol-resistant cells were highly resistant at lower concentrations, but not at higher concentrations.

The differences between the two taxol-resistant cell lines may be explained by the differences in the methodology used to create them. The tax-resistant cell line was treated with successive increasing doses of taxol until a maximum tolerated dose of 6.6 nm was reached (Guo et al., 2004). In contrast, the resistant clone was grown at an initial concentration of 7.5 μM taxol, followed by long-term incubation at 1 μM . As a result, the tax-resistant line was highly resistant at concentrations less or equal to 0.01 μM , while the clone had resistant properties at concentrations up to at least 10 μM . Because these two cell lines were distinct in their properties, it is quite possible that they express different genes and their resistant phenotypes function through different mechanisms. Indeed, genetic variability in apoptosis regulatory genes has been shown to contribute to variability in drug response (Fulda et al., 2003). As a result, both cell lines were used to compare the efficacy of liposomal taxol in comparison to conventional taxol, and more precisely delineate whether liposomal encapsulation of taxol could confer enhance chemotherapeutic effects of taxol to both taxol-resistant cell lines.

Liposomes composed of the lipids DPPC, DSPC, DMPC and DMPG were characterized with regards to their average size, taxol encapsulation efficiency, stability, and toxicity. The liposomes used in our studies were small unilamellar liposomes with an average diameter of approximately 156 nm (Figure 17). Liposomes of this size are readily taken up by cells by diffusion, allowing for efficient delivery of their contents (Figure 7; Hashimoto et al., 1992). Results from stability studies showed that DPPC-DMPG liposomes can be stored in a dehydrated powder form for months at a temperature

of -20°C (Figure 16). Upon rehydration, this formulation of liposomal taxol is highly stable in phosphate buffer when stored at 4°C, as >95% of taxol was still encapsulated after 4 days (Figure 15). The results from these studies indicate that our liposomal formulation would be suitable for use in the clinic, as the drug can be shipped and stored in dehydrated form, then rehydrated when ready for administration. Furthermore, cytotoxicity studies showed that the liposomes themselves are non-toxic to cells, even at high doses (Figure 18). These results suggest that this formulation would be safe for delivery of taxol *in vivo*.

Flow cytometric analysis of the cell cycle of the 3 MCF-7 cell lines demonstrated that liposomal taxol was able to cause increased G₂/M arrest at earlier treatment periods than conventional treatment (Figures 19a,b,c). Furthermore, an increase in the number of sub-G₁ or apoptotic cells was seen following prolonged incubation (5-7 days) with liposomal taxol when compared to conventional taxol treatment. Similar effects were seen in three MCF-7 cell lines (Tables 6a,b,c). Results from these studies have also shown that mitotic arrest is an early effect of taxol in the cells, and it is ultimately indicative of imminent cell death (Moos and Fitzpatrick, 1998). This process is accelerated by liposomal delivery of the drug. Determination of mitotic indexes was utilized to compare the amount of mitotic arrest induced by the two taxol formulations, and to confirm results of flow cytometry data. In all three MCF-7 cell lines examined, the percentage of mitotic arrest was lower than the percentage of G₂/M arrest as determined by flow cytometry. Mitotic indexes correlated with flow cytometry data in all cases. These results can be used to distinguish between the population of cells in G₂

versus the population of cells in mitotic arrest that are destined for apoptosis as determined by flow cytometry.

Degraded or sub-G₁ DNA was used as an indicator of apoptosis in flow cytometry studies (Huang et al., 1995). DNA fragmentation assays following liposomal or conventional taxol treatment were carried out on the three MCF-7 cell lines as another measure of apoptosis, and to confirm results obtained through flow cytometric analysis of the cell cycle. Results of the DNA fragmentation assay were reflective of the number of floating cells, as these were the cells isolated for analysis. The inherent number of floating or dead cells in normal, untreated culture conditions varied between the three strains of MCF-7 cells, which can partially be accounted for by cell doubling times. As a result, the values for total DNA fragmentation must also take into account the cell doubling time and individual growth characteristics of the culture. DNA fragmentation was significantly increased in a taxol-resistant clone cell line, which also had the shortest doubling time, and therefore, the highest number of cells at the end-point of the assay. Results for wild-type and tax-resistant MCF-7 cells were not as prominent, likely due to their slower growth rates and lower number of floating cells (Figure 21a,b).

To compare the uptake of the two taxol formulations and to correlate intracellular drug concentrations with effectiveness of treatment, UPLC analysis was carried out on three MCF-7 cell lines. Taxol levels from cell lysates exposed to liposomal taxol were higher than those observed following exposure to conventional taxol. Furthermore, the levels of taxol in the media isolated from cell cultures challenged with liposomal taxol or conventional taxol were lower in those cell cultures challenged with liposomal taxol (Figure 22, Table 8). These data suggest that cells with the greatest

uptake of taxol had the lowest concentrations of the drug remaining in the media. These findings also correlate with results of mitotic arrest and cell killing, suggesting that increased uptake is responsible for the increased effects on these cells.

The taxol-resistant MCF-7 cells were further characterized to elucidate the mechanism of resistance. With regards to growth rates, the tax-resistant MCF-7 cells were shown to have a significantly slower growth rate than the parental cells from which they were derived. Similar results were also reported by Li et al., 2004, as drug-resistant ovarian carcinoma cell lines were shown to have longer doubling times than their parental derivatives. Slower growth rates would allow the cells to decrease their metabolism, thereby decreasing their uptake of the drug, and possibly evading cell death. However, the taxol-resistant clone had a shorter doubling time than the wild-type cells. This suggests that an alternate mechanism of resistance is functioning in these cells, as they are not evading death by simply slowing their uptake of the drug.

Western blot analysis was used to determine if taxol-resistant MCF-7 cells overexpressed the P-glycoprotein, coded by the resistance gene MDR1, as this is one of the most commonly-reported mechanisms of resistance (Gottesman et al., 2002; Nakagawa et al., 1992; Trock et al., 1997). It was determined that one of the two resistant cell lines (tax-resistant) over-expressed the P-gp membrane pump, which correlates with results found by the group that initially donated the cell line (Guo et al., 2004). This particular cell line also had a slower doubling time, suggesting that a combination of slow uptake and drug efflux are responsible for the resistance phenotype. Overall, this study demonstrated the ability of liposomal-encapsulation of taxol to partially bypass efflux from the cell by this protein membrane pump.

The taxol-resistant MCF-7 clone did not over-express the P-gp membrane pump, suggesting that an alternate mechanism is responsible for the resistance in these cells. Results from this study indicate that this clone is only highly resistant to taxol at high concentrations of the drug ($>1 \mu\text{M}$), suggesting a possible mechanism of resistance that is induced by taxol treatment. Further study would be needed to precisely elucidate the mechanism of resistance displayed by these cells.

In order to validate the usefulness of liposomal taxol in the treatment of cancer, the effects of liposomal taxol and conventional taxol were compared on another cancer cell type, A549 lung cancer cells, as lung cancer is commonly treated with taxol (Monzo et al., 1999; Rosell et al., 2003; Seve et al., 2005; Shi et al., 2007; Yeh et al., 2003). These cells are sensitive to taxol treatment, and have a sequence of cell killing similar to that of MCF-7 cells that takes place upon treatment with the drug. Upon taxol treatment, these cells enter mitotic arrest at early time-points, followed by cell death and DNA degradation. Preliminary results presented here (Figure 27, Tables 10, 11) indicate that liposomal encapsulation of taxol provides a slight advantage in delivery of the drug in comparison to the conventional formulation. However, the difference between the two formulations is not as significant as that observed in the MCF-7 breast cancer cells.

This anomaly can be explained by the inherent differences between the two cell lines, which may be the result of the expression of different genes and proteins within the cells. It has been shown that significantly altered gene expression in cancer cells compared to normal tissue was largely tissue specific (Richardson et al., 2005; Villeneuve et al., 2006). As a result, liposomal encapsulation of taxol may improve delivery in one cell line, but not in another. Studies on alternate lung and breast cancer

cell lines may demonstrate different effects upon treatment with any formulation of taxol, depending on the individual characteristics of the cells.

Overall, results from flow cytometric analysis of the cell cycle, UPLC determination of cellular uptake of taxol, DNA fragmentation gels, and determination of mitotic indexes, conclude that liposomal encapsulation of taxol improves delivery and cytotoxic effects of the drug, in breast cancer cells cultured *in vitro*, at least partially overcoming the resistance mechanisms in these cells. The characteristics of this liposomal formulation, as conferred by its stability, high encapsulation efficiency, small particle diameter, and ability to deliver high levels of taxol within cells, might be of use in the treatment of breast cancer. Further studies in experimental animals are warranted in order to characterize the effectiveness of this formulation *in vivo*.

VIII. Future Directions

Based on the results of this project, further study of this new formulation of liposomal taxol is warranted. Future experiments should focus on the effects of liposomal taxol on different cell types that would commonly be treated with the drug, such as ovarian cancer, and different types of breast and lung cancer cells. In addition, liposomal taxol must be tested to determine its safety, pharmacokinetics and pharmacodynamics *in vivo*. If these studies were to be successful and determine that this new formulation of liposomal taxol is safe and effective for use on human patients, phase I clinical trials would then need to be performed on a small number of human patients. Prior to the commercial use of this drug, it would also need to pass through phase II and phase III clinical trials. However, because taxol is already widely used, and the liposomes are made of naturally-occurring, non-immunogenic lipids, it seems highly likely that there would be few novel side effects or toxicities associated with this new formulation. In fact, this new formulation should alleviate many of the side effects associated with the Cremophor EL (CrEL) vehicle that is currently used to deliver taxol.

IX. Conclusion

The results of this *in vitro* study have demonstrated that liposomal encapsulation of taxol can improve delivery of the drug over the conventional formulation. This new liposomal formulation, composed of the non-toxic, naturally-occurring lipids DMPG and DPPC, is able to cause increased mitotic arrest, DNA degradation, and cell death at earlier time-points in MCF-7 breast cancer cells than its conventional counterpart. Improved cell killing was correlated to increase uptake of the drug. Liposomal encapsulation of taxol also allowed the drug to partially overcome resistance mechanisms in two separate taxol-resistant MCF-7 cell lines. These results suggest that future studies on this new formulation are warranted. Specifically, it should be tested *in vivo* to complete pre-clinical trials.

List of Abbreviations

ABI-007 – Abraxane
ABC – ATP-binding cassette
ATCC – American Tissue Culture Collection
ATP – adenosine triphosphate
Bcl-2 – B-cell leukemia 2
BMS – Bristol Myers Squibb
BRCA1 – Breast cancer gene 1
BrDU – bromodeoxyuracil
CrEL (Cremophor EL) – polyethoxylated castor oil
DAB – 10-deacetylbaaccatin III
DAPI - 4',6-diamindino-2 phenylindole
DFS – Disease-free survival
DMEM – Dulbecco's Modified Eagle's Medium
DMPC - Dimyristoyl-phosphadtidylcholine
DMPG - dimyristoyl phosphatidylglycerol
DMSO – dimethyl sulfoxide
DPPC - dimyristoyl phosphatidylcholine
DSPC - Disaturated-phosphatidylcholine
ECM – extracellular matrix
EGFR – epidermal growth factor receptor
EPR effect – enhanced permeability and retention effect
FACS – fluorescence automated cell sorter
FBS – fetal bovine serum
FDA – Food and Drug Administration
G1 – gap 1 phase
G2 – gap 2 phase
HPLC – high performance liquid chromatography
HSF-55 – Human dermal fibroblast cells
IgM - immunoglobulins
MDR1 – multidrug resistance 1

M-phase – mitosis
MT1-MMP – membrane type 1 matrix metalloproteinase
MTT - 3-(4,5-Dimethylthiazol-2-yl)-2,5-diphenyltetrazolium bromide
NB – nuclei buffer
NCI – National Cancer Institute
ND – not determined
OS – overall survival
PBS – phosphate buffered saline
PCS – photon correlation spectroscopy
PEG – polyethylene glycol
P-gp – P-glycoprotein
PI-3 – phosphatidylinositol 3' kinase
PMP22 – peripheral myelin protein 22
RECIST – Response Evaluation Criteria in Solid Tumours
S – synthesis phase
SDS -PAGE– sodium dodecyl sulphate polyacrylamide gel electrophoresis
siRNAs – small interfering RNAs
Taxol – paclitaxel
t-BME – tert-butylmethyl ether
UPLC – ultra-performance liquid chromatography
UV – ultraviolet
WHO – World Health Organization

Appendix A: Buffers and Solutions

Phosphate Buffered Saline (PBS) (10X) 7.4 (1L) 80g NaCl 2g KCl 2g $\text{KH}_2\text{PO}_4 \cdot 2\text{H}_2\text{O}$ Fill up to 1L with DDW	Nuclei buffer (NB) 100ml: 8.6g sucrose (0.25M) 1.16g NaCl (0.2M) 1ml 1M Tris-HCl pH 8.0 (10mM) 0.2ml 1M MgCl_2 (2mM) 0.1ml 1M CaCl_2 (1mM) 4ml 25% TritonX-100 (1%) Fill up to 100mL with DDW. Sterilize in autoclave Store at 4°C
Propidium Iodide (PI) (50ml) 50ml 1X PBS 50ug/ml RNase 50uL of 5mg/ml stock PI Makes 5ug/ml solution Keep at 4°C and protected from light	MTT (5mg/ml) (40ml) 0.2g MTT 40ml DDW Syringe Filter Store at 4°C and protected from light
10% APS 0.1g Ammonium persulfate 1ml water	Mounting Medium (1ml) 1mg ρ -phenylenediamine (anti-fade) 100uL 1 X PBS 900uL glycerol Store at 4°C and protected from light
10X Running Buffer (1L) 144g Glycine 30.3g Tris Base 50ml 10% SDS	1X Running Buffer (1L) 900ml water 100ml 10X running buffer
10X Transfer buffer (1L) 144g Glycine 30.3g Tris base	1X Transfer Buffer (1L) 700ml water 200ml methanol 100ml 10X transfer buffer
10X TBS 30.3g Tris Base 87.6g Sodium Chloride	1X TBST 900ml water 100ml 10X TBS 1ml Tween 20
Developing Solution #1 17.7ml Water 2ml 1M Tris HCl (pH 8.5) 88uL p-Coumaric Acid	Developing Solution #2 18ml Water 2ml 1M Tris HCl (pH 8.5) 12uL Hydrogen Peroxide

200uL Luminol

Luminol (10mL)

0.44g Luminol

10ml DMSO

10% SDS-Polyacrylamide Gel (10mL)

2.5mL 40% Acrylamide

2.5mL 1.5M Tris-HCl (pH 8.8)

100uL 10% SDS

4.85mL Water

5uL TEMED

50uL 10% APS

1.3% agarose gel (30ml)

0.4g Seakem agarose

30ml 1 X TBE

p-Coumaric Acid (10ml)

0.15g p-Coumaric Acid

10ml DMSO

Stacking Gel (5mL)

0.5ml 40% Acrylamide

1.26mL 1.5M Tris-HCl (pH 6.8)

50uL 10% SDS

3.18mL Water

Freezing medium

50% FBS

43% medium

7% DMSO

1X TBE

100ml 10X TBE

900ml DDW

References

- Albumin-bound paclitaxel improves response rate vs docetaxel in metastatic breast cancer.(2007). *Oncology (Williston Park, N.Y.)*, 21(1), 109.
- Andreu, JM, Barasoain, I. (2001). The interaction of baccatin iii with the taxol binding site of microtubules determined by a homogeneous assay with fluorescent taxoid. *Biochemistry*, 40, 11975-11984.
- Atobe, K., Ishida, T., Ishida, E., Hashimoto, K., Kobayashi, H., Yasuda, J., et al. (2007). In vitro efficacy of a sterically stabilized immunoliposomes targeted to membrane type 1 matrix metalloproteinase (MT1-MMP). *Biological & pharmaceutical bulletin*, 30(5), 972-978.
- Au, J. L., Kumar, R. R., Li, D., & Wientjes, M. G. (1999). Kinetics of hallmark biochemical changes in paclitaxel-induced apoptosis. *AAPS pharmSci*, 1(3), E8.
- Bernsdorff, C., Reszka, R., & Winter, R. (1999). Interaction of the anticancer agent taxol (paclitaxel) with phospholipid bilayers. *Journal of Biomedical Materials Research*, 46(2), 141-149.
- Bhalla, K. N. (2003). Microtubule-targeted anticancer agents and apoptosis. *Oncogene*, 22(56), 9075-9086.

- Calastretti, A., Bevilacqua, A., Ceriani, C., Vigano, S., Zancai, P., Capaccioli, S., et al. (2001). Damaged microtubules can inactivate BCL-2 by means of the mTOR kinase. *Oncogene*, 20(43), 6172-6180.
- Campbell, R. B., Balasubramanian, S. V., & Straubinger, R. M. (2001). Influence of cationic lipids on the stability and membrane properties of paclitaxel-containing liposomes. *Journal of pharmaceutical sciences*, 90(8), 1091-1105.
- Carmichael, J., DeGraff, W. G., Gazdar, A. F., Minna, J. D., & Mitchell, J. B. (1987). Evaluation of a tetrazolium-based semiautomated colorimetric assay: Assessment of radiosensitivity. *Cancer research*, 47(4), 943-946.
- Ceruti, M., Crosasso, P., Brusa, P., Arpicco, S., Dosio, F., & Cattel, L. (2000). Preparation, characterization, cytotoxicity and pharmacokinetics of liposomes containing water-soluble prodrugs of paclitaxel. *Journal of controlled release : official journal of the Controlled Release Society*, 63(1-2), 141-153.
- Chiu, G. N., Abraham, S. A., Ickenstein, L. M., Ng, R., Karlsson, G., Edwards, K., et al. (2005). Encapsulation of doxorubicin into thermosensitive liposomes via complexation with the transition metal manganese. *Journal of controlled release : official journal of the Controlled Release Society*, 104(2), 271-288.
- Colombo, N., & Gore, M. (2007). Treatment of recurrent ovarian cancer relapsing 6-12 months post platinum-based chemotherapy. *Critical reviews in oncology/hematology*,

- Cragg, G. (1999). Paclitaxel (taxol®): A success story with valuable lessons for natural product drug discovery and development. *Medicinal Research Reviews*, 18(5), 315-331.
- Crosasso, P., Ceruti, M., Brusa, P., Arpicco, S., Dosio, F., & Cattel, L. (2000). Preparation, characterization and properties of sterically stabilized paclitaxel-containing liposomes. *Journal of controlled release : official journal of the Controlled Release Society*, 63(1-2), 19-30.
- Donehower, R. C. (1996). The clinical development of paclitaxel: A successful collaboration of academia, industry and the national cancer institute. *The oncologist*, 1(4), 240-243.
- Duan, Z., Brakora, K. A., & Seiden, M. V. (2004). Inhibition of ABCB1 (MDR1) and ABCB4 (MDR3) expression by small interfering RNA and reversal of paclitaxel resistance in human ovarian cancer cells. *Mol.Cancer.Ther.*, 3(7), 833-838.
- Elbayoumi, T. A., Pabba, S., Roby, A., & Torchilin, V. P. (2007). Antinucleosome antibody-modified liposomes and lipid-core micelles for tumor-targeted delivery of therapeutic and diagnostic agents. *Journal of Liposome Research*, 17(1), 1-14.
- Erasmus, J. J., Gladish, G. W., Broemeling, L., Sabloff, B. S., Truong, M. T., Herbst, R. S., et al. (2003). Interobserver and intraobserver variability in measurement of non-small-cell carcinoma lung lesions: Implications for assessment of tumor response. *Journal of clinical oncology : official journal of the American Society of Clinical Oncology*, 21(13), 2574-2582.

- Ferguson, M. R., Rojo, D. R., Somasunderam, A., Thiviyanathan, V., Ridley, B. D., Yang, X., et al. (2006). Delivery of double-stranded DNA thioaptamers into HIV-1 infected cells for antiviral activity. *Biochemical and biophysical research communications*, 344(3), 792-797.
- Ferlini, C., Ojima, I., Distefano, M., Gallo, D., Riva, A., Morazzoni, P., et al. (2003). Second generation taxanes: From the natural framework to the challenge of drug resistance. *Curr.Med.Chem.Anti-Canc Agents*, 3(2), 133-138.
- Fulda, S., & Debatin, K. (2003). Apoptosis in drug response. *Current Pharmacogenomics*, 1, 9-16.
- Gehan, E. A., & Tefft, M. C. (2000). Will there be resistance to the RECIST (response evaluation criteria in solid tumors)? *Journal of the National Cancer Institute*, 92(3), 179-181.
- Gelderblom, H., Verweij, J., Nooter, K., & Sparreboom, A. (2001). Cremophor EL: The drawbacks and advantages of vehicle selection for drug formulation. *European journal of cancer*, 37(13), 1590-1598.
- Giannakakou, P., Gussio, R., Nogales, E., Downing, K. H., Zaharevitz, D., Bollbuck, B., et al. (2000). A common pharmacophore for epothilone and taxanes: Molecular basis for drug resistance conferred by tubulin mutations in human cancer cells. *Proceedings of the National Academy of Sciences of the United States of America*, 97(6), 2904-2909.

- Gottesman, M. M., Fojo, T., & Bates, S. E. (2002). Multidrug resistance in cancer: Role of ATP-dependent transporters. *Nat.Rev.Cancer.*, 2(1), 48-58.
- Goyal, P., Goyal, K., Vijaya Kumar, S. G., Singh, A., Katare, O. P., & Mishra, D. N. (2005). Liposomal drug delivery systems--clinical applications. *Acta pharmaceutica (Zagreb, Croatia)*, 55(1), 1-25.
- Green, M. R., Manikhas, G. M., Orlov, S., Afanasyev, B., Makhson, A. M., Bhar, P., et al. (2006). Abraxane, a novel cremophor-free, albumin-bound particle form of paclitaxel for the treatment of advanced non-small-cell lung cancer. *Annals of Oncology : Official Journal of the European Society for Medical Oncology / ESMO*, 17(8), 1263-1268.
- Greiner, B., Eichelbaum, M., Fritz, P., Kreichgauer, H. P., von Richter, O., Zundler, J., et al. (1999). The role of intestinal P-glycoprotein in the interaction of digoxin and rifampin. *The Journal of clinical investigation*, 104(2), 147-153.
- Guo, B., Hembruff, S. L., Villeneuve, D. J., Kirwan, A. F., & Parissenti, A. M. (2003). Potent killing of paclitaxel- and doxorubicin-resistant breast cancer cells by calphostin C accompanied by cytoplasmic vacuolization. *Breast cancer research and treatment*, 82(2), 125-141.
- Guo, B., Villeneuve, D. J., Hembruff, S. L., Kirwan, A. F., Blais, D. E., Bonin, M., et al. (2004). Cross-resistance studies of isogenic drug-resistant breast tumor cell lines support recent clinical evidence suggesting that sensitivity to paclitaxel may be

- strongly compromised by prior doxorubicin exposure. *Breast cancer research and treatment*, 85(1), 31-51.
- Harris, J. M., & Chess, R. B. (2003). Effect of pegylation on pharmaceuticals. *Nature reviews. Drug discovery*, 2(3), 214-221.
- Hashida, M., Kawakami, S., & Yamashita, F. (2005). Lipid carrier systems for targeted drug and gene delivery. *Chemical & pharmaceutical bulletin*, 53(8), 871-880.
- Hashimoto, Y., & Suzuki, S. (1992). Basic approach to application of liposomes for cancer chemotherapy. *Tohoku J Exp Med*, 168(2), 361-369.
- Hatakeyama, H., Akita, H., Ishida, E., Hashimoto, K., Kobayashi, H., Aoki, T., et al. (2007). Tumor targeting of doxorubicin by anti-MT1-MMP antibody-modified PEG liposomes. *International journal of pharmaceutics*,
- Hofheinz, R. D., Gnad-Vogt, S. U., Beyer, U., & Hochhaus, A. (2005). Liposomal encapsulated anti-cancer drugs. *Anti-Cancer Drugs*, 16(7), 691-707.
- Huang, P., Robertson, L. E., Wright, S., & Plunkett, W. (1995). High molecular weight DNA fragmentation: A critical event in nucleoside analogue-induced apoptosis in leukemia cells. *Clinical cancer research : an official journal of the American Association for Cancer Research*, 1(9), 1005-1013.
- Huang, Y., Sheikh, M. S., Fornace, A. J., Jr., & Holbrook, N. J. (1999). Serine protease inhibitor TPCK prevents taxol-induced cell death and blocks c-raf-1 and bcl-2 phosphorylation in human breast carcinoma cells. *Oncogene*, 18(23), 3431-3439.

- Hussain, S., Pluckthun, A., Allen, T. M., & Zangemeister-Wittke, U. (2006). Chemosensitization of carcinoma cells using epithelial cell adhesion molecule-targeted liposomal antisense against bcl-2/bcl-xL. *Molecular cancer therapeutics*, 5(12), 3170-3180.
- Janicke, R. U., Sprengart, M. L., Wati, M. R., & Porter, A. G. (1998). Caspase-3 is required for DNA fragmentation and morphological changes associated with apoptosis. *The Journal of biological chemistry*, 273(16), 9357-9360.
- Jordan, M. A., & Wilson, L. (2004). Microtubules as a target for anticancer drugs. *Nature Reviews Cancer*, 4(April), 253-265.
- Kamath, K., Wilson, L., Cabral, F., & Jordan, M. A. (2005). BetaIII-tubulin induces paclitaxel resistance in association with reduced effects on microtubule dynamic instability. *The Journal of biological chemistry*, 280(13), 12902-12907.
- Kamazawa, S., Kigawa, J., Kanamori, Y., Itamochi, H., Sato, S., Iba, T., et al. (2002). Multidrug resistance gene-1 is a useful predictor of paclitaxel-based chemotherapy for patients with ovarian cancer. *Gynecologic oncology*, 86(2), 171-176.
- Kavanagh, J. J., Gershenson, D. M., Choi, H., Lewis, L., Patel, K., Brown, G. L., et al. (2005). Multi-institutional phase 2 study of TLK286 (TELCYTA, a glutathione S-transferase P1-1 activated glutathione analog prodrug) in patients with platinum and paclitaxel refractory or resistant ovarian cancer. *International journal of gynecological cancer : official journal of the International Gynecological Cancer Society*, 15(4), 593-600.

- Kennedy, R. D., Quinn, J. E., Mullan, P. B., Johnston, P. G., & Harkin, D. P. (2004). The role of BRCA1 in the cellular response to chemotherapy. *Journal of the National Cancer Institute*, 96(22), 1659-1668.
- Lafarge, S., Sylvain, V., Ferrara, M., & Bignon, Y. J. (2001). Inhibition of BRCA1 leads to increased chemoresistance to microtubule-interfering agents, an effect that involves the JNK pathway. *Oncogene*, 20(45), 6597-6606.
- Lamendola, D. E., Duan, Z., Yusuf, R. Z., & Seiden, M. V. (2003). Molecular description of evolving paclitaxel resistance in the SKOV-3 human ovarian carcinoma cell line. *Cancer research*, 63(9), 2200-2205.
- Lee, C. H., & Macgregor, P. F. (2004). Using microarrays to predict resistance to chemotherapy in cancer patients. *Pharmacogenomics*, 5(6), 611-625.
- Li, L., Luan, Y., Wang, G., Tang, B., Li, D., Zhang, W., et al. (2004). Development and characterization of five cell models for chemoresistance studies of human ovarian carcinoma. *International journal of molecular medicine*, 14(2), 257-264.
- Massing, U., & Fuxius, S. (2000). Liposomal formulations of anticancer drugs: Selectivity and effectiveness. *Drug Resist Updat*, 3(3), 171-177.
- Maur, M., & Sessa, C. (2007). Review: New biological insights in early clinical studies. *Hematological oncology*, 25(2), 53-57.

- Michieli, M., Damiani, D., Ermacora, A., Masolini, P., Michelutti, A., Michelutti, T., et al. (1999). Liposome-encapsulated daunorubicin for PGP-related multidrug resistance. *British journal of haematology*, *106*(1), 92-99.
- Miller, M. L., & Ojima, I. (2001). Chemistry and chemical biology of taxane anticancer agents. *Chemical record (New York, N.Y.)*, *1*(3), 195-211.
- Molineux, G. (2002). Pegylation: Engineering improved pharmaceuticals for enhanced therapy. *Cancer treatment reviews*, *28 Suppl A*, 13-16.
- Montgomery, R. B., Guzman, J., O'Rourke, D. M., & Stahl, W. L. (2000). Expression of oncogenic epidermal growth factor receptor family kinases induces paclitaxel resistance and alters beta-tubulin isotype expression. *Journal of Biological Chemistry*, *275*(23), 17358-17363.
- Monzo, M., Rosell, R., Sanchez, J. J., Lee, J. S., O'Brate, A., Gonzalez-Larriba, J. L., et al. (1999). Paclitaxel resistance in non-small-cell lung cancer associated with beta-tubulin gene mutations. *Journal of clinical oncology : official journal of the American Society of Clinical Oncology*, *17*(6), 1786-1793.
- Moos, P. J., & Fitzpatrick, F. A. (1998). Taxanes propagate apoptosis via two cell populations with distinctive cytological and molecular traits. *Cell growth & differentiation : the molecular biology journal of the American Association for Cancer Research*, *9*(8), 687-697.
- Morin, P. J. (2003). Drug resistance and the microenvironment: Nature and nurture. *Drug Resist Updat*, *6*(4), 169-172.

- Mross, K., Niemann, B., Massing, U., Dreves, J., Unger, C., Bhamra, R., et al. (2004). Pharmacokinetics of liposomal doxorubicin (TLC-D99; myocet) in patients with solid tumors: An open-label, single-dose study. *Cancer chemotherapy and pharmacology*, 54(6), 514-524.
- Nakagawa, M., Schneider, E., Dixon, K. H., Horton, J., Kelley, K., Morrow, C., et al. (1992). Reduced intracellular drug accumulation in the absence of P-glycoprotein (mdr1) overexpression in mitoxantrone-resistant human MCF-7 breast cancer cells. *Cancer research*, 52(22), 6175-6181.
- National Cancer Institute. (2006). *Drug discovery at the national cancer institute: Fact sheet*. Retrieved June, 2007, from <http://www.cancer.gov/cancertopics/factsheet/NCIdrugdiscovery>
- Nolte, T., Kaufmann, W., Schorsch, F., Soames, T., & Weber, E. (2005). Standardized assessment of cell proliferation: The approach of the RITA-CEPA working group. *Experimental and toxicologic pathology : official journal of the Gesellschaft fur Toxikologische Pathologie*, 57(2), 91-103.
- Nunez, R. (2001). DNA measurement and cell cycle analysis by flow cytometry. *Current Issues in Molecular Biology*, 3(3), 67-70.
- Ofir, R., Seidman, R., Rabinski, T., Krup, M., Yavelsky, V., Weinstein, Y., et al. (2002). Taxol-induced apoptosis in human SKOV3 ovarian and MCF7 breast carcinoma cells is caspase-3 and caspase-9 independent. *Cell death and differentiation*, 9(6), 636-642.

- Padhani, A. R., & Husband, J. E. (2000). Commentary. are current tumour response criteria relevant for the 21st century? *The British journal of radiology*, 73(874), 1031-1033.
- Pakunlu, R. I., Cook, T. J., & Minko, T. (2003). Simultaneous modulation of multidrug resistance and antiapoptotic cellular defense by MDR1 and BCL-2 targeted antisense oligonucleotides enhances the anticancer efficacy of doxorubicin. *Pharmaceutical research*, 20(3), 351-359.
- Park, J. O., Lee, S. I., Song, S. Y., Kim, K., Kim, W. S., Jung, C. W., et al. (2003). Measuring response in solid tumors: Comparison of RECIST and WHO response criteria. *Japanese journal of clinical oncology*, 33(10), 533-537.
- Park, S. J., Wu, C. H., Gordon, J. D., Zhong, X., Emami, A., & Safa, A. R. (2004). Taxol induces caspase-10-dependent apoptosis. *The Journal of biological chemistry*, 279(49), 51057-51067.
- Pecheur, E. I., Lavillette, D., Alcaras, F., Molle, J., Boriskin, Y. S., Roberts, M., et al. (2007). Biochemical mechanism of hepatitis C virus inhibition by the broad-spectrum antiviral arbidol. *Biochemistry*, 46(20), 6050-6059.
- Potter, A. J., Gollahon, K. A., Palanca, B. J., Harbert, M. J., Choi, Y. M., Moskovitz, A. H., et al. (2002). Flow cytometric analysis of the cell cycle phase specificity of DNA damage induced by radiation, hydrogen peroxide and doxorubicin. *Carcinogenesis*, 23(3), 389-401.

- Richardson, A., & Kaye, S. B. (2005). Drug resistance in ovarian cancer: The emerging importance of gene transcription and spatio-temporal regulation of resistance. *Drug Resist Updat*, 8(5), 311-321.
- Rosell, R., Scagliotti, G., Danenberg, K. D., Lord, R. V., Bepler, G., Novello, S., et al. (2003). Transcripts in pretreatment biopsies from a three-arm randomized trial in metastatic non-small-cell lung cancer. *Oncogene*, 22(23), 3548-3553.
- Schmidt, M., Lu, Y., Liu, B., Fang, M., Mendelsohn, J., & Fan, Z. (2000). Differential modulation of paclitaxel-mediated apoptosis by p21Waf1 and p27Kip1. *Oncogene*, 19(20), 2423-2429.
- Schyth, B. D., Lorenzen, N., & Pedersen, F. S. (2007). A high throughput in vivo model for testing delivery and antiviral effects of siRNAs in vertebrates. *Molecular therapy : the journal of the American Society of Gene Therapy*, 15(7), 1366-1372.
- Sengupta, S., Tyagi, P., Chandra, S., Kochupillai, V., & Gupta, S. K. (2001). Encapsulation in cationic liposomes enhances antitumour efficacy and reduces the toxicity of etoposide, a topo-isomerase II inhibitor. *Pharmacology*, 62(3), 163-171.
- Seve, P., Mackey, J., Isaac, S., Tredan, O., Souquet, P. J., Perol, M., et al. (2005). Class III beta-tubulin expression in tumor cells predicts response and outcome in patients with non-small cell lung cancer receiving paclitaxel. *Mol.Cancer.Ther.*, 4(12), 2001-2007.
- Shi, A., An, T., Zhu, G., Yu, R., Xu, G., Liu, X., et al. (2007). Phase I study to determine the MTD of paclitaxel given three times per week during concurrent radiation

therapy for stage III non-small cell lung cancer. *Current medical research and opinion*, 23(5), 1161-1167.

Sinico, C., De Logu, A., Lai, F., Valenti, D., Manconi, M., Loy, G., et al. (2005).

Liposomal incorporation of artemisia arborescens L. essential oil and in vitro antiviral activity. *European journal of pharmaceutics and biopharmaceutics : official journal of Arbeitsgemeinschaft fur Pharmazeutische Verfahrenstechnik e.V.*, 59(1), 161-168.

Soepenbergh, O., Sparreboom, A., de Jonge, M. J., Planting, A. S., de Heus, G., Loos, W.

J., et al. (2004). Real-time pharmacokinetics guiding clinical decisions; phase I study of a weekly schedule of liposome encapsulated paclitaxel in patients with solid tumours. *European journal of cancer*, 40(5), 681-688.

Sparreboom, A., Scripture, C. D., Trieu, V., Williams, P. J., De, T., Yang, A., et al.

(2005). Comparative preclinical and clinical pharmacokinetics of a cremophor-free, nanoparticle albumin-bound paclitaxel (ABI-007) and paclitaxel formulated in cremophor (taxol). *Clinical cancer research : an official journal of the American Association for Cancer Research*, 11(11), 4136-4143.

Sparreboom, A., van Zuylen, L., Brouwer, E., Loos, W. J., de Bruijn, P., Gelderblom, H.,

et al. (1999). Cremophor EL-mediated alteration of paclitaxel distribution in human blood: Clinical pharmacokinetic implications. *Cancer research*, 59(7), 1454-1457.

- Sugimura, M., Sagae, S., Ishioka, S., Nishioka, Y., Tsukada, K., & Kudo, R. (2004). Mechanisms of paclitaxel-induced apoptosis in an ovarian cancer cell line and its paclitaxel-resistant clone. *Oncology*, *66*(1), 53-61.
- Szakacs, G., Paterson, J. K., Ludwig, J. A., Booth-Genthe, C., & Gottesman, M. M. (2006). Targeting multidrug resistance in cancer. *Nat.Rev.Drug Discov.*, *5*(3), 219-234.
- Theodoulou, M., & Hudis, C. (2004). Cardiac profiles of liposomal anthracyclines: Greater cardiac safety versus conventional doxorubicin? *Cancer*, *100*(10), 2052-2063.
- Trock, B. J., Leonessa, F., & Clarke, R. (1997). Multidrug resistance in breast cancer: A meta-analysis of MDR1/gp170 expression and its possible functional significance. *Journal of the National Cancer Institute*, *89*(13), 917-931.
- Turco, L., De Angelis, I., Stamatii, A., & Zucco, F. (2000). Apoptosis evaluation in epithelial cells exposed to different chemicals: Relevance of floating cells. *Cell biology and toxicology*, *16*(1), 53-62.
- Tzafiriri, A. R., Lerner, E. I., Flashner-Barak, M., Hinchcliffe, M., Ratner, E., & Parnas, H. (2005). Mathematical modeling and optimization of drug delivery from intratumorally injected microspheres. *Clinical cancer research : an official journal of the American Association for Cancer Research*, *11*(2 Pt 1), 826-834.

- van Tellingen, O., Huizing, M. T., Panday, V. R., Schellens, J. H., Nooijen, W. J., & Beijnen, J. H. (1999). Cremophor EL causes (pseudo-) non-linear pharmacokinetics of paclitaxel in patients. *British journal of cancer*, *81*(2), 330-335.
- Villeneuve, D. J., Hembruff, S. L., Veitch, Z., Cecchetto, M., Dew, W. A., & Parissenti, A. M. (2006). cDNA microarray analysis of isogenic paclitaxel- and doxorubicin-resistant breast tumor cell lines reveals distinct drug-specific genetic signatures of resistance. *Breast cancer research and treatment*, *96*(1), 17-39.
- Vyas, S. P., Rawat, M., Rawat, A., Mahor, S., & Gupta, P. N. (2006). Pegylated protein encapsulated multivesicular liposomes: A novel approach for sustained release of interferon alpha. *Drug development and industrial pharmacy*, *32*(6), 699-707.
- Wang, Y., O'Brate, A., Zhou, W., & Giannakakou, P. (2005). Resistance to microtubule-stabilizing drugs involves two events: Beta-tubulin mutation in one allele followed by loss of the second allele. *Cell cycle (Georgetown, Tex.)*, *4*(12), 1847-1853.
- Wang, Z., Butt, K., Wang, L., & Liu, H. (2007). The effect of seal oil on paclitaxel induced cytotoxicity and apoptosis in breast carcinoma MCF-7 and MDA-MB-231 cell lines. *Nutrition and cancer*, *58*(2), 230-238.
- Wierenge, D. I., & Eaton, C. R. (2007). *Phases of product development*. Retrieved June, 2007, from http://www.allp.com/drug_dev.htm
- Williams, J., Lucas, P. C., Griffith, K. A., Choi, M., Fogoros, S., Hu, Y. Y., et al. (2005). Expression of bcl-xL in ovarian carcinoma is associated with chemoresistance and recurrent disease. *Gynecologic oncology*, *96*(2), 287-295.

- Yano, T., Itoh, Y., Matsuo, M., Kawashiri, T., Egashira, N., & Oishi, R. (2007). Involvement of both tumor necrosis factor-alpha-induced necrosis and p53-mediated caspase-dependent apoptosis in nephrotoxicity of cisplatin. *Apoptosis : An International Journal on Programmed Cell Death*,
- Yeh, J. J., Hsu, W. H., Wang, J. J., Ho, S. T., & Kao, A. (2003). Predicting chemotherapy response to paclitaxel-based therapy in advanced non-small-cell lung cancer with P-glycoprotein expression. *Respiration; international review of thoracic diseases*, 70(1), 32-35.
- Yeh, T. K., Lu, Z., Wientjes, M. G., & Au, J. L. (2005). Formulating paclitaxel in nanoparticles alters its disposition. *Pharmaceutical research*, 22(6), 867-874.
- Yonemoto, H., Ogino, S., Nakashima, M. N., Wada, M., & Nakashima, K. (2007). Determination of paclitaxel in human and rat blood samples after administration of low dose paclitaxel by HPLC-UV detection. *Biomedical chromatography : BMC*, 21(3), 310-317.
- Yowell, S. L., & Blackwell, S. (2002). Novel effects with polyethylene glycol modified pharmaceuticals. *Cancer treatment reviews*, 28 Suppl A, 3-6.
- Zou, Y., Fu, H., Ghosh, S., Farquhar, D., & Klostergaard, J. (2004). Antitumor activity of hydrophilic paclitaxel copolymer prodrug using locoregional delivery in human orthotopic non-small cell lung cancer xenograft models. *Clinical cancer research : an official journal of the American Association for Cancer Research*, 10(21), 7382-7391.

